PHYSICAL REVIEW D **91,** 125003 (2015)

Multimeson Yukawa interactions at criticality

Gian Paolo Vacca*
INFN, Sezione di Bologna, via Irnerio 46, I-40126 Bologna, Italy

Luca Zambelli†
Theoretisch-Physikalisches Institut, Friedrich-Schiller-Universität Jena, D-07743 Jena, Germany
(Received 8 April 2015; published 1 June 2015)

The critical behavior of a relativistic $\mathbb{Z}_2$-symmetric Yukawa model at zero temperature and density is discussed for a continuous number of fermion degrees of freedom and of spacetime dimensions, with emphasis on the role played by multimeson exchange in the Yukawa sector. We argue that this should be generically taken into account in studies based on the functional renormalization group, either in four-dimensional high-energy models or in lower-dimensional condensed-matter systems. By means of the latter method, we describe the generation of multicritical models in less than three dimensions, both at infinite and finite numbers of flavors. We also provide different estimates of the critical exponents of the chiral Ising universality class in three dimensions for various field contents, from a couple of massless Dirac fermions down to the supersymmetric theory with a single Majorana spinor.

DOI: 10.1103/PhysRevD.91.125003 PACS numbers: 11.10.Kk, 11.30.Qc, 71.27.+a, 71.30.+h

I. INTRODUCTION

In this paper we will study the renormalization group (RG) flow of a simple Yukawa model describing relativistic fermions interacting through the exchange of scalar fluctuations. We will discuss some of its critical properties in a continuum of spacetime dimensions $2 < d \leq 4$, dedicating most of the analysis to the $d = 3$ case. The class of models we want to consider is described by the generic bare Lagrangian

$$\mathcal{L} = \frac{1}{2}\partial^\mu\phi\partial_\mu\phi + V(\phi) + \bar{\psi}\gamma^\mu i\partial_\mu\psi + iH(\phi)\bar{\psi}\psi, \quad (1.1)$$

where we have N_f copies of fermions, the representation of which will be kept general in the following, and one real scalar field. The requirement of power-counting renormalizability would further restrict the interactions inside the potentials V and H (and would generically require the inclusion of derivative interactions, too), but we are not going to impose such conditions, since we are interested in describing the possible conformal models in this family, even if strongly coupled. In case the potentials V and H are even and odd, respectively, the system is characterized by a chiral $\mathbb{Z}_2$ symmetry, besides the $\mathrm{U}(N_f)$ symmetry. For this reason, the model with bare potentials

$$V(\phi) = \frac{\bar{m}^2}{2}\phi^2 + \frac{\bar{\lambda}_2}{2}\phi^4, \qquad H(\phi) = \bar{y}\phi \quad (1.2)$$

is often called the Gross–Neveu–Yukawa model, since it shares these symmetries with the purely fermionic Gross–Neveu model [1] and can be obtained from it by means of a Hubbard–Stratonovich transformation.

Even for more general bare Lagrangians that are not related by any bosonization technique, the Yukawa models and chiral fermionic models remain deeply connected. The three-dimensional Gross–Neveu model shows a second-order quantum phase transition that separates the phase with preserved chiral symmetry from the one where this is spontaneously broken and a chiral condensate of fermions appears. The latter can be effectively described as a scalar degree of freedom, and therefore this transition can be unveiled also as a dynamical effect in interacting scalar-spinor systems. Indeed, it is found that the critical properties of the Gross–Neveu model in $2 < d < 4$ dimensions are compatible with the ones of the Yukawa model, thus indicating that the two are in the same universality class, which for a generic but nonvanishing flavor number is also called the chiral Ising universality class. In both parametrizations, this is described by a non-Gaussian fixed point (FP) of the RG flow. As a consequence, nonperturbative tools are best suited for the investigation of its properties and for the extraction of key quantities such as the corresponding critical exponents. Indeed several methods have been applied to this problem, including ϵ expansions [2–6], large-N_f expansions [4,7,8], lattice simulations [9–13], and functional RG equations [14–19].

These critical properties have great physical relevance for the description of several systems. Three-dimensional relativistic fermionic systems, appear in several interesting condensed matter problems. For instance, QED and the Thirring model in $2 + 1$ dimensions have been considered for theories of high-T_C superconductivity [20]. Concerning the description of electrons in graphene, one can make use of slight variants of these lower-dimensional models [21],

*vacca@bo.infn.it
†luca.zambelli@uni-jena.de

 © 2015 American Physical Society

as well as of theories in which gauge fields can propagate out of the plane [22]. Understanding the phase diagram and critical properties of these models at variable N_f represents pretty much the same challenge as the one posed by the Gross–Neveu and Yukawa models, and one can even address them in a unified picture [23]. Even the simple Yukawa model discussed in this work can find applications to extremely nontrivial phenomena in condensed matter. For the case of two massless Dirac fermions, its quantum critical phase transition in $d = 3$ might be a close relative of the putative transition between the semimetallic and the Mott-insulating phases of electrons in graphene [18]. For a single Dirac field instead, it is considered to be in the same universality class of spinless fermions on the honeycomb lattice with repulsive nearest neighbors interactions [13].

For a single Majorana spinor, it is a precious example of a three-dimensional model showing emergent supersymmetry. Indeed, it is known that in this case the critical theory not only enjoys $\mathcal{N} = 1$ supersymmetry but also possesses only one relevant component, which means that by tuning a single macroscopic parameter one can discriminate between two distinct phases with preserved or spontaneously broken supersymmetry [17,24]. On these grounds, a potential experimental realization of supersymmetry was proposed in Ref. [24], at the boundary of topological superconductors. A similar phenomenon occurs for Yukawa systems with complex scalars and spinors, which have been argued to give rise to an emergent $\mathcal{N} = 2$ supersymmetry [25].

The phase diagram of Gross–Neveu and Yukawa models has been analysed in $d < 4$ also for a better understanding of their $d \to 4$ limit. Clearly, nonperturbative phenomena in the latter case can have many applications in particle physics. These range from the chiral phase transition in QCD [26], where these models serve as simplified versions of quark-meson models [27], to the Higgs sector of the standard model [28,29] and to toy models of composite-Higgs extensions [30].

In the present work, we will analyze a more general truncation scheme for the functional renormalization group (FRG) study of these systems, showing under which conditions this brings important improvements in the results obtained by means of the latter nonperturbative method. Such a truncation scheme amounts to allowing for a generic potential $H(\phi)$, that essentially describes vertices with two fermions and an arbitrary number of scalars. This kind of interactions has been neglected in the FRG studies of fermionic models for a long time. Only recently have they been discussed in other works considering more complicated models and different but related questions. For example, in Ref. [31] the flow equations for this Yukawa system coupled to quantum gravity were derived, but only the linear coupling $H(\phi) = \bar{y}\phi$ was considered in explicit studies of these equations. Most prominently, in Ref. [32] the effect of higher Yukawa couplings on the chiral phase structure of QCD at finite temperature and chemical potential was analyzed by means of an effective quark-meson model. It was observed, within polynomial truncations of a Yukawa potential $H(\phi)$, that higher-order quark-meson interactions are quantitatively important in the description of the chiral transition.

A similar but different study will be performed here, for the present $\mathbb{Z}_2$-symmetric Yukawa model, in lower dimensionality and for a generic number of flavors. We will confine ourselves to the study of the zero-temperature system at criticality, looking for scaling solutions for various d and N_f and comparing the results obtained with different methods. In Sec. III we start with the leading order of the $1/N_f$ expansion, reproducing known results in three dimensions and generalizing them to multicritical theories below three dimensions. Technical details regarding this analysis are sketched in Appendix B. In Sec. IV we turn to a finite number of fermions and, by neglecting the wave function renormalization of the fields, we observe how critical Yukawa theories arise while continuously lowering the dimensionality toward 2. To this end, we consider the FP equations for the two generic functions $V(\phi)$ and $H(\phi)$ and solve them numerically without resorting to any truncation. In Sec. V, still neglecting the wave function renormalizations, we adopt a different strategy for the numerical integration of the FP equations and compute the global FP potentials in three dimensions, for various flavor numbers. For the case of a single Majorana spinor, we also apply these numerical methods to the computation of the critical exponents and perturbations. In Sec. VI we discuss polynomial truncations, showing how these can give results in satisfactory agreement with the global numerical analysis. As a consequence, we use them for a self-consistent inclusion of the wave function renormalizations and produce estimates of the critical exponents in three dimensions and for various numbers of fermions, which we compare with some of the existing literature. Finally, in Sec. VII we address the $d \to 4$ limit at a low number of fermions, and in Sec. VIII we draw a summary of our results. Yet, to introduce our work, we need to provide the reader with the definition of the approximations involved in the computation of the flow equations, and with the resulting beta-functions. This is the object of the next section and of Appendix A.

II. RG FLOW OF A SIMPLE YUKAWA MODEL WITH MULTIMESON EXCHANGE

The FRG is a representation of quantum dynamics based on Wilson's idea of floating cutoff k. In this work we will adopt its formulation in terms of a scale-dependent one particle irreducible effective action [33], often called the average effective action. For a given system, the form of this action is determined by the field content Φ and by the symmetry properties, as well as by an initial condition (bare action) and boundary conditions for the integration of the flow equation

$$\dot{\Gamma}_k[\Phi] = \frac{1}{2}\mathrm{STr}[(\Gamma_k^{(2)}[\Phi] + R_k)^{-1}\dot{R}_k]. \tag{2.1}$$

Here $(\Gamma_k^{(2)}[\Phi] + R_k)^{-1}$ represents the matrix of regularized propagators, while R_k is a momentum-dependent masslike regulator. Since the dot stands for differentiation with respect to the RG time $t = \log k$, this flow equation comprehends the infinite set of beta-functions for the infinitely many allowed interactions inside Γ_k. Extracting them amounts to projecting both sides of the equation on each separate interaction functional. In practical computations, one drops infinitely many operators, thus performing a nonperturbative approximation called truncation of the theory space. To this end, several systematic strategies are available and appropriate in different circumstances, such as the vertex expansion or the derivate expansion. For reviews see Ref. [34].

In this work we will consider the following truncation:

$$\Gamma_k[\phi, \psi, \bar{\psi}] = \int \mathrm{d}^d x \left(\frac{1}{2} Z_{\phi,k} \partial^\mu \phi \partial_\mu \phi + V_k(\phi) + Z_{\psi,k} \bar{\psi} \gamma^\mu i \partial_\mu \psi + i H_k(\phi) \bar{\psi} \psi \right). \tag{2.2}$$

Here ϕ is a real scalar field, while ψ denotes N_f copies of a spinor field with d_γ real components. The latter parameter is related to the symmetries of the system and plays therefore a crucial role in pure fermionic as well as in fermion-boson models. Yet, as long as we truncate the theory space to the Ansatz of Eq. (2.2), focusing on the mechanism of $\mathbb{Z}_2$-symmetry breaking, we can simply deal with the total number of real Grassmannian degrees of freedom $X_f = d_\gamma N_f$, considering it as an arbitrary real number. As soon as $X_f \geq 2$, the truncation above is missing purely fermionic derivative-free interactions, that are indeed symmetry sensitive and that would contribute to the leading (zeroth) order of the derivative expansion. Furthermore, it is also missing field-dependent contributions to the wave function renormalizations Z_ϕ and Z_ψ, which would appear in the next-to-leading (first) order of the derivative expansion. In the following we will call the Ansatz of Eq. (2.2) a local potential approximation (LPA) for this simple Yukawa model, whenever the wave function renormalizations are neglected ($Z_{\phi,k} = Z_{\psi,k} = 1$), and therefore the fields have no anomalous dimensions $\eta_{\phi,\psi} = -\partial_t \log Z_{\phi,\psi}$. The inclusion of the latter will be named LPA′. Our justification for the choice of this truncation is in the exhaustive evidence that similar Ansätze give a good description of the existence and properties of conformal models in $2 < d \leq 4$ for linear systems with scalar degrees of freedom [34].

Projection of the Wetterich equation on the truncation of Eq. (2.2) yields the running of the corresponding parameters. Since we are interested in reproducing conformal models, that correspond to scaling solutions of the RG flow, it is useful to consider rescaled amplitudes

$$\phi \longrightarrow \frac{k^{(d-2)/2}}{Z_\phi^{1/2}}\phi, \qquad \psi \longrightarrow \frac{k^{(d-1)/2}}{Z_\psi^{1/2}}\psi,$$

since the new dimensionless renormalized field would then be constant at criticality. As a consequence we will focus on the potentials for these fields,

$$v_k(\phi) = k^{-d} V_k\left(\frac{Z_\phi^{1/2}\phi}{k^{(d-2)/2}}\right),$$

$$h_k(\phi) = \frac{k^{-1}}{Z_\psi} H_k\left(\frac{Z_\phi^{1/2}\phi}{k^{(d-2)/2}}\right).$$

In this new set of variables, the flow equations read

$$\dot{v} = -dv + \frac{d-2+\eta_\phi}{2}\phi v' + 2v_d\{l_0^{(\mathrm{B})d}(v'') - X_f l_0^{(\mathrm{F})d}(h^2)\} \tag{2.3}$$

$$\dot{h} = h(\eta_\psi - 1) + \frac{d-2+\eta_\phi}{2}\phi h' + 2v_d\{2h(h')^2 l_{1,1}^{(\mathrm{FB})d}(h^2, v'') - h'' l_1^{(\mathrm{B})d}(v'')\} \tag{2.4}$$

$$\eta_\phi = \frac{4v_d}{d}\{(v^{(3)})^2 m_4^{(\mathrm{B})d}(v'') + 2X_f (h')^2[m_4^{(\mathrm{F})d}(h^2) - h^2 m_2^{(\mathrm{F})d}(h^2)]\}_{\phi_0} \tag{2.5}$$

$$\eta_\psi = \frac{8v_d}{d}\{(h')^2 m_{1,2}^{(\mathrm{FB})d}(h^2, v'')\}_{\phi_0}, \tag{2.6}$$

where $v_d = (2^{d+1}\pi^{d/2}\Gamma(d/2))^{-1}$, the threshold functions $l^{(\mathrm{F/B})d}$ and $m^{(\mathrm{F/B})d}$ on the right hand side denote regulator-dependent contributions from loops containing fermionic or bosonic propagators, and the equations for the anomalous dimensions are to be evaluated at the minimum ϕ_0 of the scalar potential. Their definition can be found in Appendix A, together with the explicit form they take for the linear regulator, which is our choice in this work, since it allows for a simple analytic computation of such integrals and, for scalar $O(\mathrm{N})$ models, it optimizes the performance of truncations based on low orders of the derivative expansion [35]. For this linear regulator, the flow equations of the two potentials read

$$\dot{v} = -dv + \frac{d-2+\eta_\phi}{2}\phi v' + C_d\left(\frac{1-\frac{\eta_\phi}{d+2}}{1+v''} - X_f\frac{1-\frac{\eta_\psi}{d+1}}{1+h^2}\right) \tag{2.7}$$

$$\dot{h} = h(\eta_\psi - 1) + \frac{d-2+\eta_\phi}{2}\phi h' + C_d\left[2h(h')^2\left(\frac{1-\frac{\eta_\psi}{d+1}}{(1+h^2)^2(1+v'')} + \frac{1-\frac{\eta_\phi}{d+2}}{(1+h^2)(1+v'')^2}\right) - \frac{h''(1-\frac{\eta_\phi}{d+2})}{(1+v'')^2}\right], \tag{2.8}$$

where we have denoted for convenience $C_d = 4v_d/d$.

A simple way of facilitating the stability of the vacuum is the requirement of $\mathbb{Z}_2$ symmetry, i.e. invariance over $\phi \to -\phi$. For a standard Yukawa system, with a linear bare Yukawa interaction $H(\phi) = y\phi$, this requires a discrete chiral symmetry $\psi \to i\psi$ and $\bar{\psi} \to i\bar{\psi}$. A generalization of local interactions with such a symmetry then requires an odd $H(\phi)$. There is also the possibility to leave the spinors unchanged under the transformation, which would require an even function $H(\phi)$.

The goal of this work is to construct global FP solutions of the flow equations compatible with the symmetry conditions and to study the properties of the RG flow in their neighborhood. The FPs, which describe scaling solutions, are computed by solving the coupled system of two ordinary differential equations $\dot{v} = 0$ and $\dot{h} = 0$ or, in some cases, from the equivalent system for the quantities $(v,\ y = h^2)$. The dependence of such scaling solutions on the two parameters d and X_f is one of the main themes discussed in the literature as well as in the present work. Regarding the former, we will assume $2 < d \leq 4$ and qualitatively discuss how the number of critical models varies with d, but we will especially concentrate on the properties of the $d = 3$ system. For the latter, we restrict ourselves to a non-negative number of degrees of freedom, and we start from the two simple limiting cases one can address. The simplest is $X_f \to 0$. In this case, the fermion sector remains nontrivial, see Eqs. (2.4) and (2.6), but is not allowed to influence the scalar dynamics, which is therefore identical to the fermion-free model; see Eqs. (2.3) and (2.5). Hence, as far as criticality is concerned, we expect to observe the same pattern of FPs that can be observed without fermions, with the same critical exponents in the scalar sector, even if at generically nonvanishing values of the Yukawa couplings. The second limit which brings radical simplifications is $X_f \to \infty$, and it is discussed in the next section.

III. LEADING-ORDER LARGE $-X_f$ EXPANSION

Large-N_f methods are a traditional and successful way to analyze the strongly coupled domain of the three-dimensional Gross–Neveu model, which is renormalizable at any order in a $1/N_f$ expansion [4,7,8]. As a consequence, any other nonperturbative method is challenged to reproduce known results in this limit. For this reason, before moving to the finite-X_f results provided by the FRG, let us start with discussing the behavior of this simple Yukawa model with many fermionic degrees of freedom, within the basic parametrization of its dynamics provided by Eq. (2.2), in a continuous set of dimensions $2 < d < 4$. This FRG analysis, for the case of a linear Yukawa function, has already been performed in Ref. [16]. Our results can be considered as an extension of it, to include a generic function $h(\phi)$. As we will see, the main advantage that this brings at large X_f is the possibility to describe also multicritical models in $d < 3$.

In this section let us replace v with $X_f v$, as well as η_ϕ with $X_f\eta_\phi$, and look at the leading order in $1/X_f$. The first simplification is the fact that only canonical scaling terms and pure fermion loops survive. Therefore, the flow equations at this order reduce to

$$\dot{v} = -dv + \frac{d-2+\eta_\phi}{2}\phi v' - 2v_d l_0^{(\mathrm{F})d}(h^2) \tag{3.1}$$

$$\dot{h} = h(\eta_\psi - 1) + \frac{d-2+\eta_\phi}{2}\phi h' \tag{3.2}$$

$$\eta_\phi = \frac{4v_d}{d}(h')^2[m_4^{(\mathrm{F})d}(h^2) - 2h^2 m_2^{(\mathrm{F})d}(h^2)] \tag{3.3}$$

$$\eta_\psi = 0. \tag{3.4}$$

Let us draw some general considerations about the FP solutions, by postponing the task of consistently solving the flow equation for η_ϕ. The equation for h is almost regulator independent (apart for the value of η_ϕ), and the solution is a simple power,

$$h(\phi) = c_h\phi^{2/(d-2+\eta_\phi)}. \tag{3.5}$$

This is real only if the exponent is rational and with an odd denominator. Furthermore it is smooth only if the exponent is a positive integer. The FP solution for v is instead regulator dependent. Adopting the linear regulator, in $2 < d < 4$ it reads

$$v(\phi) = c_v \phi^{2d/(d-2+\eta_\phi)} - \frac{4v_d}{d^2}\, {}_2F_1\left(1, -\frac{d}{2}; 1-\frac{d}{2}; -h(\phi)^2\right). \tag{3.6}$$

The function ${}_2F_1(1, -\frac{d}{2}; 1-\frac{d}{2}, -x)$, which actually can be reduced to a Hurwitz–Lerch function $-\frac{d}{2}\Phi(-x, 1, -\frac{d}{2})$, has a logarithmic singularity at $x = -1$, and therefore the condition that $h(\phi)$ be real entails that this singularity is always avoided, and that the potential is globally defined. On the other hand, the smoothness of v is not taken for granted. Since

$$ {}_2F_1\left(1, -\frac{d}{2}; 1-\frac{d}{2}; -x\right) = 1 - \frac{d}{d-2}x - \frac{d}{4-d}x^2 + O(x^3) \tag{3.7}$$

and since this function is always convex, the leading ϕ dependence of v at its minimum, i.e. at the origin, is provided by $h^2(\phi)$ itself. Hence, the latter must be a smooth function because we want the couplings associated to the derivatives of the potential at the minimum to be well defined at the FP. The same reasoning, if applied to the Yukawa couplings, leads to the requirement that $h(\phi)$ be smooth at the origin. This translates into a quantization condition on the dimensionality of the scalar field

$$\frac{d-2+\eta_\phi}{2} = \frac{1}{n}, \qquad n \in \mathbb{N} \tag{3.8}$$

which is a consequence of the large-X_f limit.

We find it helpful, for the interpretation of this relation, to consider a similar condition at the purely scalar FPs, with trivial Yukawa interaction. With this we mean the limit $X_f \to \infty$ followed by $c_h \to 0$, which is clearly not the same as the fermion-free model; yet, by consistency, this limit should describe the classical properties of the latter model. Indeed, if $c_h = 0$ the only condition left is that the homogeneous part of the FP scalar potential be smooth and stable; that is

$$\frac{d-2+\eta_\phi}{2} = \frac{d}{2n}, \qquad n \in \mathbb{N}. \tag{3.9}$$

The meaning of this constraint is well known. By neglecting the quantum corrections, hence setting $\eta_\phi = 0$, one would deduce that the smooth bounded solutions $v(\phi) = c_v\phi^{2n}$ are allowed only in

$$d_n = \frac{2n}{n-1} = 2 + \frac{2}{n-1}, \qquad n \in \mathbb{N}. \tag{3.10}$$

This is the usual tree-level counting according to which the interaction ϕ^{2n} is marginal in d_n and becomes relevant for $d < d_n$. From the quantum point of view, these dimensions are the corresponding upper critical dimensions for multicritical universality classes. For any n, below d_n a new FP with nontrivial η_ϕ branches from the Gaussian FP and survives for $2 \le d < d_n$ [36,37]. In the purely scalar model, this is already visible within a simple LPA of the FRG, where it is indeed possible to unveil and describe some properties of these universality classes in a whole continuum of dimensions $2 < d < d_m$. In the leading order of the large-X_f expansion, the fact that quantum effects allow for these FPs at any $2 \le d < d_n$ remains invisible. This is because in the LPA one sets $\eta_\phi = 0$, and in the LPA′ the $c_h \to 0$ limit again forces a vanishing anomalous dimension. This simply signals that the two limits $X_f \to \infty$ and $h(\phi) \to 0$ do not commute.

A similar analysis can be applied to the Yukawa system. Namely, if one forces classical scaling and sets $\eta_\phi = 0$, the large-X_f limit constrains d to the critical values

$$d_n = 2 + \frac{2}{n}, \qquad n \in \mathbb{N} \tag{3.11}$$

that are exactly the dimensions at which the interaction terms $\phi^n\bar{\psi}\psi$ become marginal. Notice that they coincide with the critical dimensions of an even scalar potential and that by selecting odd or even functions $h(\phi)$ one can reduce the number of critical dimensions for h by a factor of 2. As soon as anomalous scaling is allowed, the large-X_f limit tells us that the nontrivial FPs can indeed exist for $d < d_n$ and quantizes the corresponding anomalous dimensions

$$\eta_\phi = \frac{2}{n} + 2 - d = d_n - d, \qquad n \in \mathbb{N}. \tag{3.12}$$

Notice that they get smaller and smaller, the closer d is to the upper critical dimension d_n. As a consequence, the value of X_f at which one expects a breakdown of the LPA with $\eta_\phi = 0$ must be a decreasing function of $(d_n - d)$. Unfortunately, the latter is maximum for the very interesting $n = 1$ scaling solution, which includes the $d = 3$ Gross–Neveu universality class. However, even in this case, for small enough X_f we have no *a priori* reason to discard the use of the LPA for a first study of the critical Yukawa models. On the other hand, for the $n = 1$ scaling solution, the LPA′ is able to reproduce Eq. (3.12) and therefore provides a consistent picture of this critical model for any X_f; see Appendix B. This is not the case for the $n > 1$ multicritical models, the nontrivial scaling properties of which require larger truncations of the FRG.

Before going on and discussing the finite-X_f results, let us comment on the universal critical exponents that one should approach in a large-X_f limit, since they provide an important reference point for the finite-X_f investigations. The eigenvalue problem for the linearized flow in vicinity of the large-X_f FPs is solved in Appendix B, both in the LPA and in the LPA′. The result is that one can safely split the problem into two classes of perturbations. The former have $\delta h(\phi) = 0$ and $\delta v(\phi) = \delta c_v \phi^M$, where we required the potential to be smooth, thus quantizing the corresponding critical exponents to the values

$$\theta_M = d - M\left(\frac{d-2+\eta_\phi}{2}\right) = d - \frac{M}{n}, \qquad M \in \mathbb{N}, \quad (3.13)$$

i.e. the dimensionality of the couplings in front of $\delta v(\phi)$. The latter have $\delta h(\phi) = \delta c_h \phi^N$, a nontrivial $\delta v(\phi)$, and again

$$\theta_N = 1 - N\left(\frac{d-2+\eta_\phi}{2}\right) = 1 - \frac{N}{n}, \qquad N \in \mathbb{N}, \quad (3.14)$$

where we used Eq. (3.8) as before. As a consequence, the large-X_f exponents are independent of c_h and c_v. They are Gaussian in the sense that they are directly linked to the dimensionality of the fields by naive dimensional counting, but the latter dimensionality, as far as the scalar is concerned, is deeply non-Gaussian and actually independent of d.

As usual one can observe a hierarchy among FPs with different n. For example, let us restrict ourselves to the slice of theory space parametrized by the couplings inside $h(\phi)$ only. Then, for a FP labelled by the integer n, there are n relevant operators, namely $\phi^0, \ldots, \phi^{n-1}$, and one marginal operator, ϕ^n itself. Within the LPA, the latter can be exactly marginal, since it corresponds to shifts in c_h. For the $n = 1$ FP, the LPA$'$ is enough to change this conclusion, since the flow equation for η_ϕ provides a condition that fixes the FP value of c_h. For $n > 1$, higher truncations are needed. Thus, the $\bar{n}$th FP can provide UV completion for theories approaching the nth FP in the IR, only if $n < \bar{n}$. The detailed study of the global flows among these FPs is in principle a straightforward task in the large-X_f approximation, but it is out of the purposes of the present work. We confine ourselves to sketching some properties of the FP potentials and of the linearized perturbations in vicinity of the FPs, which can be found in Appendix B, together with some comments on how these nontrivial critical theories disappear in $d = 4$.

IV. LPA AT FINITE X_f AND GENERIC d. SOME FEATURES FROM NUMERICAL INVESTIGATIONS

In the previous section, we described how the large-X_f expansion supports the expectation that, as the number of dimensions is lowered from $d = 4$ toward $d = 2$, across the upper critical dimensions of Eq. (3.11), new universality classes become accessible in the theory space of Yukawa models. In this section we are going to present evidence that this happens also at finite X_f. Here and in the rest of this work, we restrict our analysis to the subset of theory space which enjoys a conventional $\mathbb{Z}_2$ symmetry, such that v is even and h is odd. Furthermore we adopt the LPA and neglect the flow equations for the wave function renormalization of the fields. As it was argued in the previous section, as well as in Appendix B with more details, one cannot expect this approximation to perform well for any n and X_f. Therefore, the following studies should be understood as a first step toward a proper description of these universality classes. Only the $d = 3$ chiral Ising universality class will be later analyzed also in the LPA$'$, by resorting to polynomial truncations of the potentials; see Sec. VI.

Since we look for odd Yukawa potentials, we can restrict the list of the operators that become relevant at the corresponding critical dimensions:

$$\begin{aligned} \phi^{2n}:\ & d_c^v(n \geq 2) = \frac{2n}{n-1} = 4, 3, \frac{8}{3}, \frac{5}{2}, \frac{12}{5} \cdots \\ \phi^{2n+1}\bar{\psi}\psi:\ & d_c^h(n \geq 0) = \frac{4(n+1)}{2n+1} = 4, \frac{8}{3}, \frac{12}{5} \cdots \end{aligned} \quad (4.1)$$

To reveal the new universality classes appearing below these dimensions, we follow the strategy developed in Refs. [38,39], that has already been successfully applied to the purely scalar model in continuous dimensions [37]. This consists of solving the FP condition, which is a Cauchy problem involving a system of two coupled second-order ordinary differential equations (ODEs), by a numerical shooting method, i.e. varying the initial conditions in a space of parameters which is two dimensional, since two of the four boundary conditions are fixed by the symmetry requirements ($v'(0) = 0$ and $h(0) = 0$). For the potential v, we choose as parameter $\sigma = v''(0)$, relating it to $v(0)$ using the differential equation. For h we use $h_1 = h'(0)$. Trying to numerically solve the nonlinear differential equations with generic initial conditions, one typically encounters a singularity at some value of $\phi_c(\sigma, h_1)$ where the algorithm stops. Such a value increases in a steep way close to the initial conditions which correspond to a global solution, even if the numerical errors mask partially this behavior. As a consequence, in our case a three-dimensional plot for $\phi_c(\sigma, h_1)$ is very useful to gain a first understanding of the positions of the possible FPs.

In Fig. 1 we show the results of this analysis, for $X_f = 1$ and for several dimensions: $d = 5, 4, 3.9, 3.5, 3, \frac{8}{3}, \frac{8}{3} - \frac{1}{10}, \frac{5}{2}, \frac{12}{5}$. For $d = 5$ and $d = 4$, as it is expected, we see a single spike in $(\sigma, h_1) = (0, 0)$ which corresponds to the Gaussian solution. More details on this are given, for $X_f < 1$, in Sec. VII. In $3 < d < 4$ we have crossed the threshold below which both the operators ϕ^4 and $\phi\bar{\psi}\psi$ become relevant, as is shown in Eq. (4.1). In this interval, it is evident from the figure that we find three new spikes. One is characterized by $h_1 = 0$ and $\sigma < 0$ and corresponds to the Ising critical solution. It is clearly visible in the fourth and fifth panels of Fig. 1, but not in the third, since it is very close to the Gaussian FP. The other two are physically equivalent, since they lie at opposite values of h_1, and correspond to the chiral Ising universality class. They have $\sigma < 0$, which suggests that also these scaling solutions are in a broken

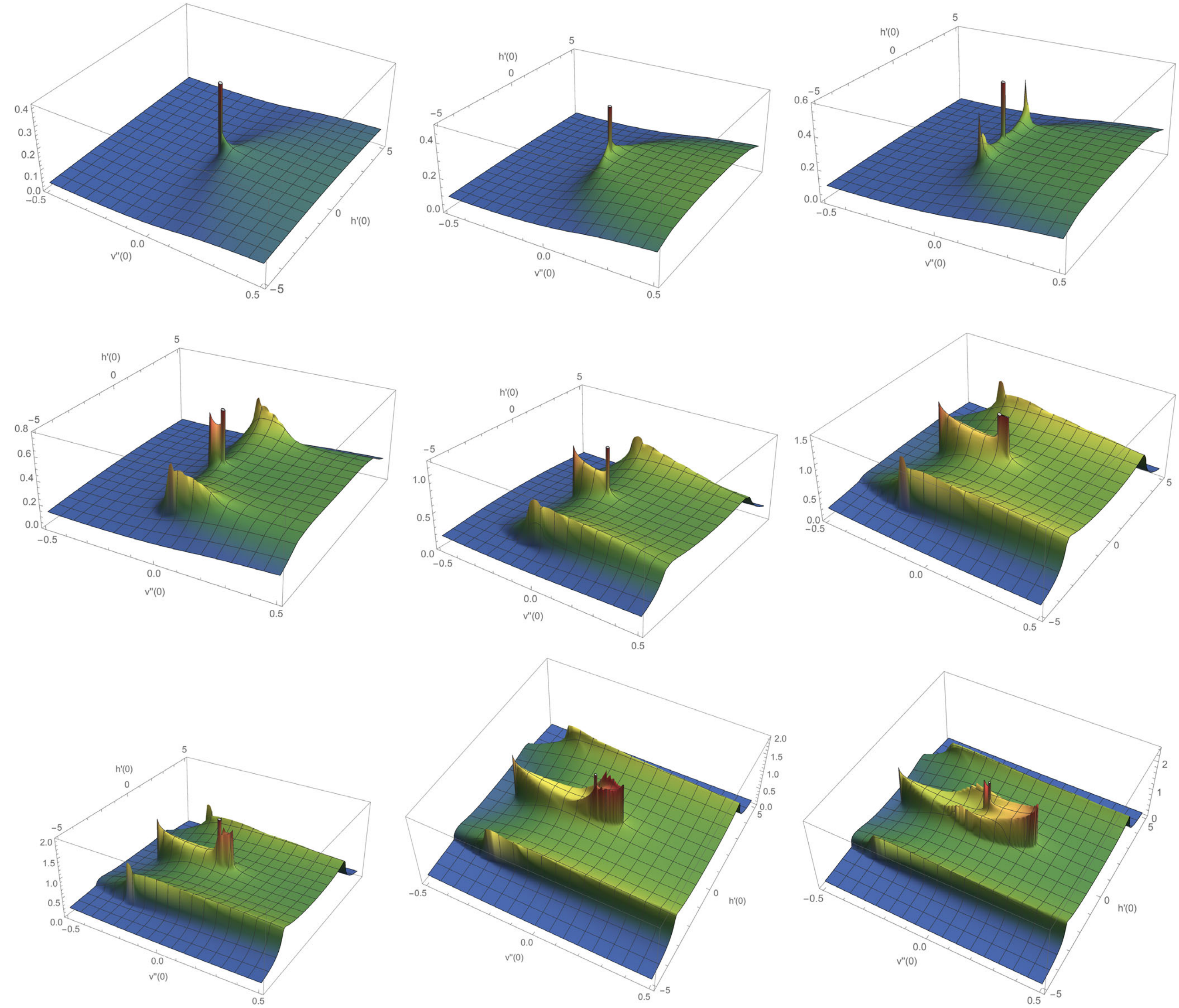

FIG. 1 (color online). Spike plots for $X_f = 1$ on varying the dimension, $d = 5, 4, 3.9, 3.5, 3, \frac{8}{3}, \frac{8}{3} - \frac{1}{10}, \frac{5}{2}, \frac{12}{5}$, from left to right and from top to bottom.

regime for $X_f = 1$, at least in the LPA approximation. Moving to $\frac{8}{3} < d < 3$ we cross the marginality threshold for the operator ϕ^6, but no other operators involving fermions have to be added to the set of the relevant ones. This corresponds to the appearance of the tricritical theory in the pure scalar sector, as we see from the new spike which develops with $\sigma > 0$ and $h_1 = 0$. Once $d < \frac{8}{3}$ also the new operators ϕ^8 and $\phi^3\bar{\psi}\psi$ become relevant, and new critical solutions may appear. Indeed, in the left and the central plots of the third line of Fig. 1, we see two new spikes, which again occur at opposite values of h_1 and are therefore equivalent, this time with $\sigma > 0$. Finally in the lower-right plot, where we present the case $d = \frac{12}{5}$, which is lower than $\frac{5}{2}$ enough to clearly see the effects of the new relevant scalar operator ϕ^8, one can appreciate the third new spike at $\sigma < 0$ and $h_1 = 0$. The latter FP corresponds to the quadricritical scalar model as described for example in Refs. [37,40]. The former solutions, already assuming that they globally exist, define what one could call the chiral quadricritical Ising universality class, since they originate from the Gaussian FP together with the purely scalar quadricritical model.

We do not show more plots with lower values of d, since the pattern is pretty clear. Pushing further this analysis toward dimensions close to $d = 2$, though conceptually straightforward, would probably anyway require more than the LPA. To provide the reader with some more details, in Fig. 2 we zoom in the panel of Fig. 1 that refers to $d = \frac{8}{3} - \frac{1}{10}$. The three nontrivial spikes which appeared at higher values of $d > 3$ are now out of this graph. From this figure one can see with more accuracy the presence of the three new nontrivial solutions. The two of them which lie at

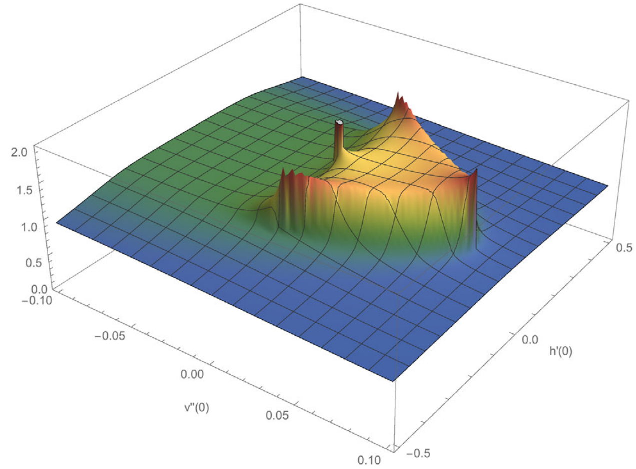

FIG. 2 (color online). Spike plot for $d=\frac{8}{3}-\frac{1}{10}$ and $X_f=1$, zoomed area around the origin.

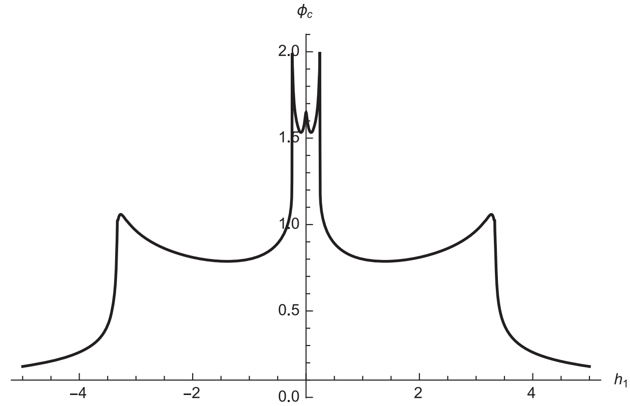

FIG. 3. Spike plot for $d=\frac{8}{3}-\frac{1}{10}$ and $X_f=1$, zoomed area around the origin.

$h_1 \neq 0$ can also be visualized by a plot at constant value of σ, approximately corresponding to the position of the peaks; see Fig. 3. Here the range of h_1 is wider than in Fig. 2, so that one can see also a trace of the FPs generated at $d<4$, which are nevertheless located at a different value of σ.

The analysis we discussed in this section can be repeated for other values of X_f, thus getting a qualitative understanding of the position of the FPs as a function of both d and X_f. However, because of the uncertainties in the location of these peaks, it is hard to get a good qualitative knowledge of this function. Nevertheless, the latter is needed to prove that the arguments presented in this section are rigorous, that each of the peaks corresponds to one FP, and to compute the corresponding critical exponents. For this reason, in the next section, we are going to adopt a different numerical method that will allow us to precisely answer these questions, focusing on $d=3$ for definiteness, but allowing for a generic X_f.

V. $d=3$ LPA AT FINITE X_f. NUMERICAL SOLUTION OF THE FP EQUATIONS

In this section we construct, for some specific cases, the numerical solutions for v and h of the FP differential equations, obtained by setting Eqs. (2.7) and (2.8) equal to zero, in a domain for the dimensionless field ϕ that covers the asymptotic region. This is what might be called a global scaling solution. For convenience, we have actually considered the equivalent system for the quantities $v(\phi)$ and $y(\phi)=h^2(\phi)$. We focus here on $d=3$ for which, from the analysis at $X_f=1$ performed in the previous section, we expect a FP with nontrivial scalar potential and Yukawa function. In the following we are going to take several values of X_f into account. After having found the corresponding nontrivial FP potentials, we determine the associated critical exponents and eigenperturbations. The knowledge of the global scaling solutions will be important for a study of the quality of polynomial expansions, presented in Sec. VI. The latter approach is very useful especially in the case of the LPA′, which gives us access to a self-consistent computation of the anomalous dimensions without enlarging the truncation to a full next-to-leading order of the derivative expansion. Clearly this programmatic analysis can be repeated for other values of d.

We choose to construct a global numerical solution by starting from the knowledge of the asymptotic behavior allowed by the FP equations. Once the asymptotic expansions are determined with sufficient accuracy, we proceed, with a shooting method, to the numerical integration from the asymptotic region toward the origin. The properties of the solutions which reach the origin depend on the free parameters in the asymptotic expansions. By requiring the solutions to transform correctly under $\mathbb{Z}_2$, one can uniquely fix the latter parameters to their FP values [41]. The leading term of the asymptotic expansion for both v and h is determined, in the LPA with vanishing anomalous dimensions, by the classical scaling. Here we report the first correction to it. Denoting $\alpha=2/(d-2)$, the asymptotic behavior of the solution of the FP equations in the LPA reads

$$v_{\mathrm{asympt}}(\phi) \simeq A\phi^{2\alpha+2} + \phi^{-2\alpha}\frac{C_d(B-2AX_f(\alpha+1)(2\alpha+1))}{2AB(\alpha+1)(2\alpha+1)(d+2)} + \cdots$$
$$h^2_{\mathrm{asympt}}(\phi) \simeq B\phi^{2\alpha} + \phi^{-2-2\alpha}\frac{C_d\alpha(4\alpha(2\alpha+1)A+B)}{2A^2(\alpha+1)(2\alpha+1)^2(d+2)} + \cdots \qquad (5.1)$$

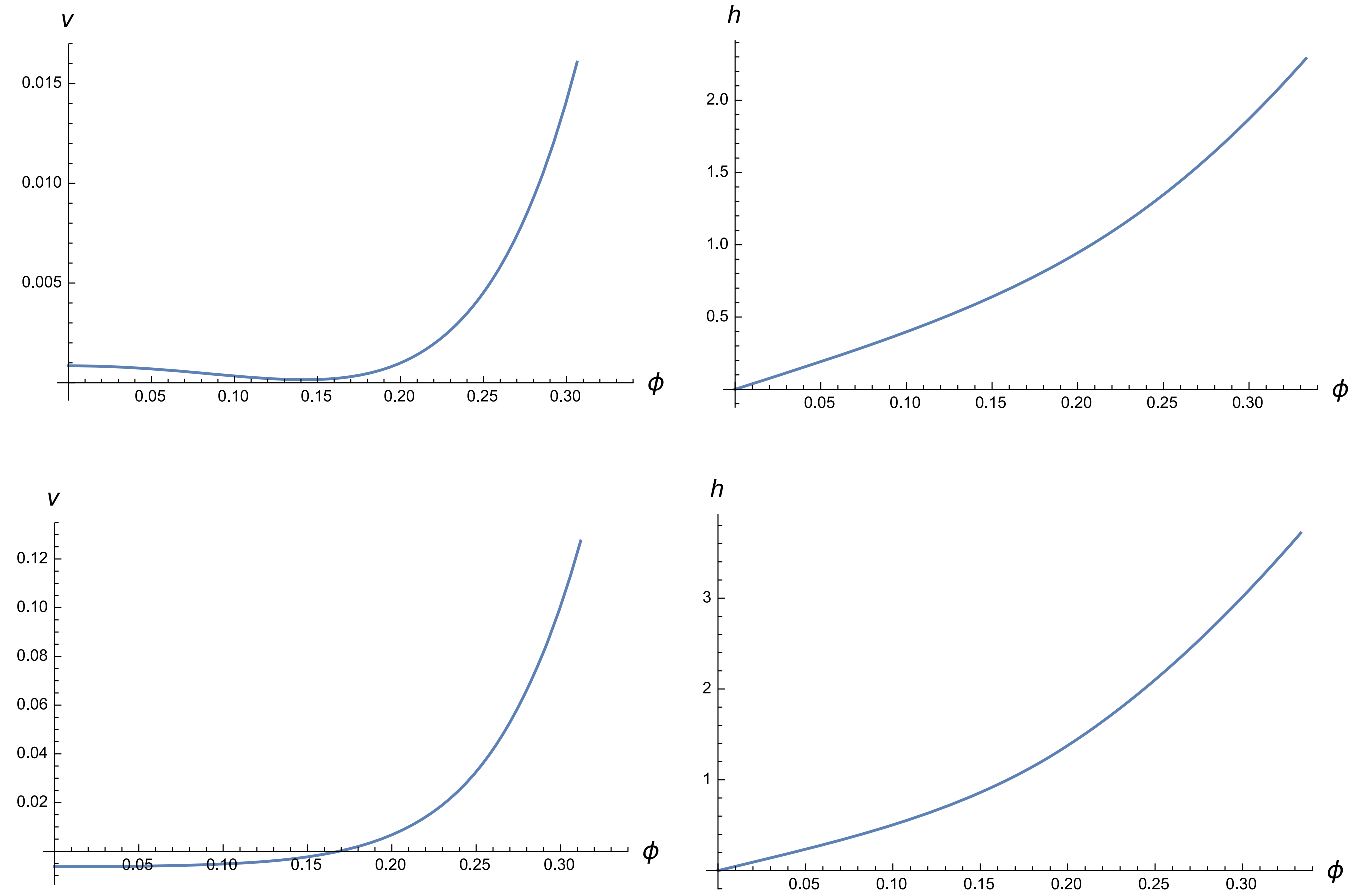

FIG. 4 (color online). The potentials v and h at the global scaling solution, computed numerically within the LPA. The case $X_f = 1$, which is in the broken regime, appears in the first two panels (top), while $X_f = 2$, in the symmetric regime, is shown in the last two panels (bottom).

and depends on two real parameters A and B. In our analysis we have computed and used asymptotic expansions with eight terms for each potential. Starting the numerical evolution from some large value for $\phi = \phi_{\mathrm{max}}$, we have then investigated $v'(0)$ and $h(0)$ as functions of A and B. Computing numerically the gradient of these two functions, we were able to employ a kind of Newton–Raphson method to determine their zeros, i.e. the values of A and B corresponding to $\mathbb{Z}_2$-symmetric scaling solutions. In Fig. 4 we present two examples of

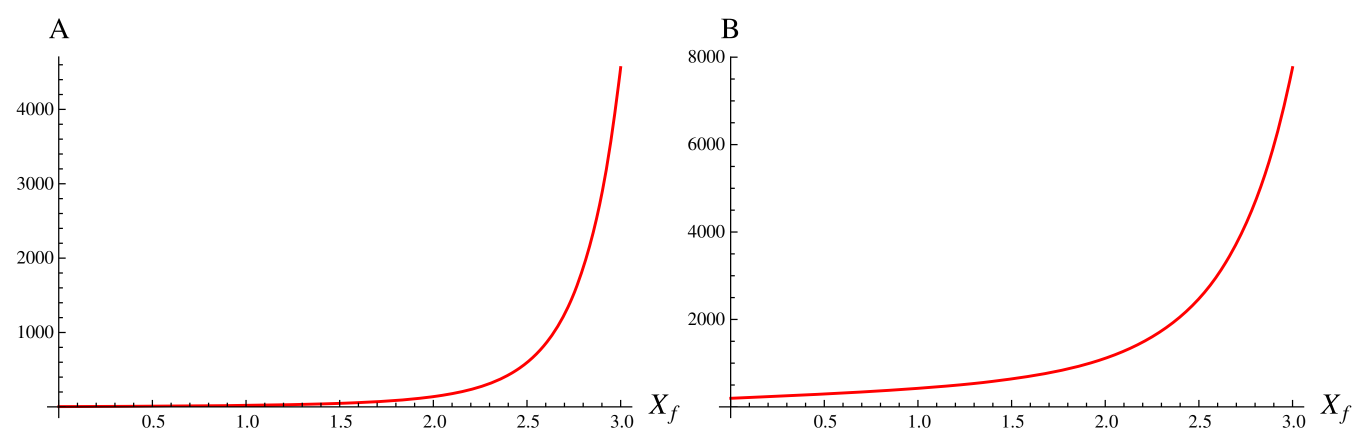

FIG. 5 (color online). The values of the asymptotic parameters (A,B) defined by Eq. (5.1) at the scaling solutions, varying X_f in the range $10^{-3} < X_f < 3$.

global solutions for the cases $X_f = 1$ and $X_f = 2$. The former is in the broken regime, since the $\mathbb{Z}_2$ symmetric scalar potential has a nontrivial minimum, while the latter is in the symmetric regime. Any solution (v, h) is characterized by two parameters, such as for example A and B, or $v''(0)$ and $h'(0)$, which indeed fix completely the Cauchy problem once they are complemented by the symmetry conditions. In Fig. 5 we show the FP values of the integration constants A and B as defined by Eq. (5.1). The locus of the FP solutions in the plane $[v''(0), h'(0)]$ as a function of $X_f \in [10^{-3}, 3]$ is instead presented in Fig. 6. Notice that as X_f approaches zero, in the lower left end of the curve, $h'(0)$ attains a finite value, which is situated around 3.3. It is evident that the two regimes, broken and symmetric, are realized in two complementary intervals of X_f. The transition between the two occurs at $X_f \simeq 1.64$ for the LPA. In the next section, we will see that this value is slightly modified in the LPA′ and becomes $X_f \simeq 1.62$. The vacuum expectation value ϕ_0 and the value of $h'(\phi_0)$ as functions of X_f are presented in Fig. 7.

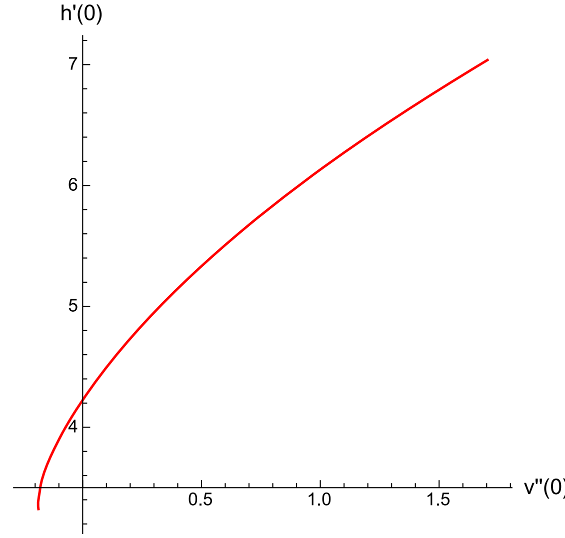

FIG. 6 (color online). The values of $(v''(0), h'(0))$ from the numerical global scaling solutions, varying X_f in the range $10^{-3} < X_f < 3$. One can notice the transition from the broken to the symmetric regime, which occurs at $X_f \simeq 1.64$ for the present LPA.

The critical exponents of these scaling solutions and the corresponding eigenperturbations are an important piece of information. This is obtained by studying the evolution of the small perturbations around the FPs. Therefore, the linearized flow equations are the main tool to study such a problem. They are constructed, taking advantage of the separation of variables in ϕ and k, by substituting into the flow equations

$$\begin{aligned} v_k(\phi) &= v^*(\phi) + \epsilon \delta v(\phi) e^{\lambda t}, \\ y_k(\phi) &= y^*(\phi) + \epsilon \delta y(\phi) e^{\lambda t} \end{aligned} \tag{5.2}$$

and then keeping the first term in ϵ, for $\epsilon \ll 1$. Such a procedure leads to the eigenvalue problem

$$\begin{aligned} 0 = {} & (\lambda - d)\delta v + \frac{1}{2}(d-2)\phi \delta v' \\ & + C_d\left(\frac{X_f}{(1+y)^2}\delta y - \frac{1}{(1+v'')^2}\delta v''\right) \end{aligned} \tag{5.3}$$

and

$$\begin{aligned} 0 = {} & (\lambda - 2)\delta y + \left(\frac{d}{2} - 1\right)\phi \delta y' + C_d\Bigg[\delta v'' \frac{(2y(y+1)^2 y'' - (y')^2(y(v''+5) + 3y^2 + 1))}{y(1+y)^2(1+v'')^3} \\ & - \delta y (y')^2\left(\frac{2}{(1+y)^3(v''+1)} + \frac{(3y^2+2y+1)}{2y^2(1+y)2(1+v'')^2}\right) \\ & + \delta y' y'\left(\frac{2}{(1+y)^2(1+v'')} + \frac{(3y+1)}{y(1+y)(1+v'')^2}\right) - \frac{\delta y''}{(1+v'')^2}\Bigg], \end{aligned} \tag{5.4}$$

where for simplicity we have renamed v^* and y^* as v and y. This system is of the form

$$(\hat{O} - \lambda)\delta f = 0, \tag{5.5}$$

if δf is the vector of perturbations, $\delta f^T = (\delta v, \delta y)$, and $\hat{O}$ is the corresponding differential operator. We have considered two different ways to solve this eigenvalue problem.

The first approach is a direct generalization of the one we have already discussed for scaling solutions, in this case applied to the full set of equations: FP plus linearized flow. The asymptotic behavior of the eigenperturbations is computed by solving the asymptotic form of the linearized equations for a large field, which is obtained using the known asymptotic expansion for v and y at the FP, given in Eq. (5.1). In $d = 3$ one finds

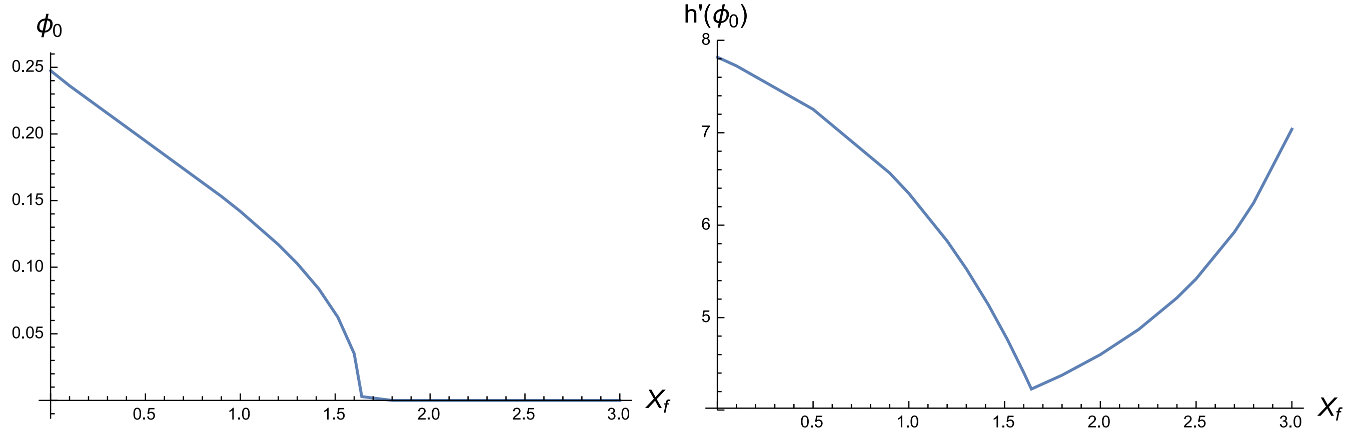

FIG. 7 (color online). The vacuum expectation value $\phi_0(X_f)$ from the numerical global scaling solutions is shown in the left panel, while in the right panel, we plot the corresponding value of $h'(\phi_0)(X_f)$, both in the LPA.

$$\delta v_{\mathrm{asympt}} = \phi^{6-2\lambda} + \phi^{-2\lambda-4}\frac{(450A^2\beta X_f + B^2(-2\lambda^2+11\lambda-15))}{13500\pi^2A^2B^2} + \mathcal{O}(\phi^{-8-2\lambda})$$
$$\delta y_{\mathrm{asympt}} = \beta\phi^{4-2\lambda} - \phi^{-2\lambda-6}\left(\frac{(2\lambda^2-11\lambda+15)(20A+B)}{16875\pi^2A^3} + \frac{\beta(240A\lambda + B(2\lambda^2+5\lambda-6))}{13500\pi^2A^2B}\right) + \mathcal{O}(\phi^{-10-2\lambda}). \tag{5.6}$$

In practice we used an asymptotic expansion with up to three terms per perturbation. We note that in a linear homogeneous problem the overall normalization of the eigenvector δf plays no role. Therefore, the asymptotic form of δf depends only on a relative real parameter β, which we choose to be a constant multiplying the leading term of δy. One more free parameter is needed for tuning the behavior of the solutions at the origin, such that they fulfill the symmetry requirements $\delta v'(0) = 0$ and $\delta y(0) = 0$. This can be interpreted as the eigenvalue λ itself. As a consequence, one expects a discrete spectrum of allowed values for λ and β. Unfortunately, due to numerical uncertainties, with this method we have been able only to restrict the eigenvalues to an interval described by a continuous function $\lambda(\beta)$. Indeed one has to remember that the global numerical solutions have been constructed on some bounded neighborhood of the origin, even if the latter overlaps with the region where the large field asymptotic behavior becomes dominant. Moreover, the linearized equations depend on derivatives of the numerical global FP solutions, for which the accuracy is reduced.

The second approach we considered consists of inserting the known numerical FP solutions in the linearized equations, computing a numerical expression for all the ϕ-dependent coefficients of this eigenvalue problem and then solving them by means of a pseudospectral method based on Chebyshev polynomials. Also in this case, some uncertainties remain, for the same reasons mentioned above. As an example, for $X_f = 1$ the leading critical exponent we find is $\theta_1 = -\lambda_1 = 1.2279$, which refers to the only relevant direction (we do not consider $\theta_0 = 3$, since it is related to an additive constant in the potential and it is unphysical in flat space). All the other eigenvalues λ_i are positive and associated to irrelevant operators, for instance $\theta_2 = -\lambda_2 = -0.6236$ and $\theta_3 = -\lambda_3 = -1.5842$. The relevant direction corresponds to the eigenperturbation $\delta f_1 = (\delta v, \delta h)$ shown in Fig 8. Notice the fact that the relevant eigenpertubation has $\delta h(\phi) \neq 0$ unlike in the large-X_f analysis, where the only relevant perturbation compatible with symmetry requirements is $\delta v(\phi) = \delta c_v \phi^2$, which corresponds to $\theta_1 = 1$. Even if $X_f = 1$ is quite away from this limit, it is know that in this case the FP theory is a $\mathcal{N} = 1$ Wess–Zumino model [17,24] and that the supersymmetry-preserving relevant perturbation is a change in the mass of the scalar field [17,42], which therefore leaves the Yukawa sector unchanged. Hence, $\delta h \neq 0$ is probably a consequence of the explicit breaking of supersymmetry introduced by our regularization scheme.

We do not push further here the spectral analysis of the critical exponents and associated perturbations as a function of X_f, leaving it for a future study based on algorithms giving better control on the numerical errors. In the present work, these global numerical computations at $X_f = 1$ will serve as a reference for the development of a different, local, approximation method, based on polynomial truncations of the functions $v(\phi)$ and $h(\phi)$. The latter will be discussed in the next section and will be also used for a more reliable discussion of the dependence of the critical exponents on the number of fermion degrees of freedom.

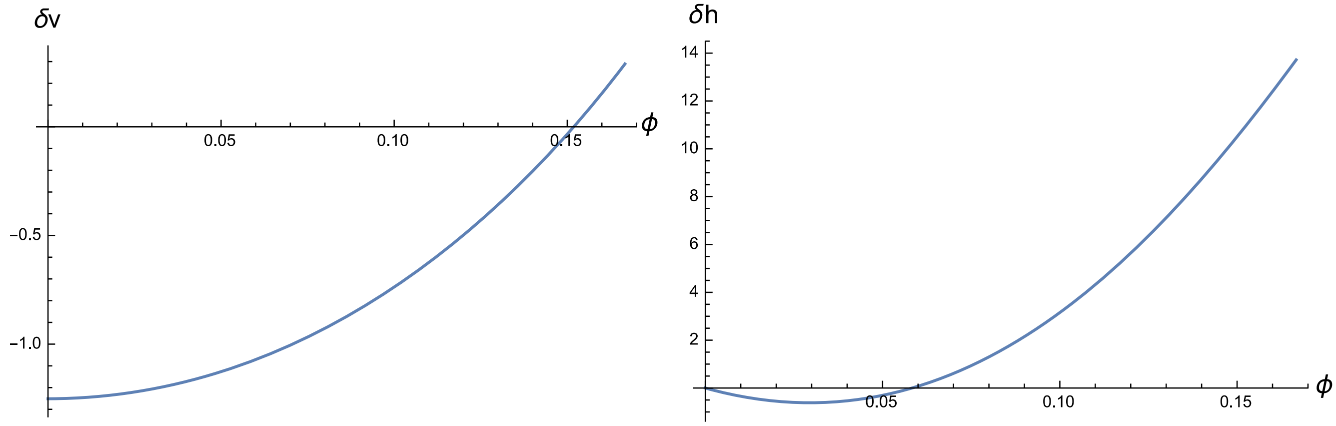

FIG. 8 (color online). Case $d = 3$ and $X_f = 1$: the components δv and δh of the relevant eigenperturbation, from the global numerical analysis of the LPA.

VI. POLYNOMIAL ANALYSIS IN $d = 3$

In this section we are going to discuss the use of polynomial parametrizations and consequent truncations of the functions $v(\phi)$ and $h(\phi)$. Though for definiteness we will address the specific case of the unique $d = 3$ nontrivial critical Yukawa theory, similar techniques can be applied to the other scaling solutions in $2 < d < 3$, presumably with the same degree of success. Section VI A will present results obtained within the LPA, which can be directly compared to the full functional analysis developed in the previous section. This will make us confident about the effectiveness and soundness of polynomial truncations, as well as of the necessity to go beyond a simple linear Yukawa coupling for an accurate description of critical properties of the theory. On these grounds, Sec. VI B will push forward the analysis to a self-consistent inclusion of the wave function renormalization of the fields, which is essential for quantitative estimates of the critical exponents, which will be compared with some literature for several values of X_f. Polynomial truncations will be also used in Sec. VII for some comments on the four-dimensional model.

Let us start by presenting the truncation schemes we are going to analyze. Since we restrict ourselves to $d = 3$, we will demand $v(\phi)$ and $h(\phi)$ to be even and odd, respectively. We will use the common notation $\rho = \phi^2/2$, and we will adopt only one name for one and the same quantity, regardless of whether it is considered as a function of ϕ or as a function of ρ. In the symmetric regime, the physically meaningful parametrization of the scalar potential is a Taylor expansion around vanishing field

$$v(\rho) = \sum_{n=0}^{N_v} \frac{\lambda_n}{n!}\rho^n. \tag{6.1}$$

Regarding the Yukawa potential, we are interested in two possible Taylor expansions, one for $h(\phi)$, already adopted in Ref. [32], and one for $y(\rho) = [h(\phi)]^2$. In the symmetric regime, they read

$$h(\phi) = \phi \sum_{n=0}^{N_h-1} \frac{h_n}{n!}\rho^n \tag{6.2}$$

$$y(\rho) = \sum_{n=1}^{N_h} \frac{y_n}{n!}\rho^n. \tag{6.3}$$

In the regime of spontaneous symmetry breaking (SSB), the potential $v(\rho)$ develops a nontrivial minimum $\kappa = \phi_0^2/2$, which becomes the preferred reference point for a different Taylor expansion,

$$v(\rho) = \lambda_0 + \sum_{n\geq 2}^{N_v} \frac{\lambda_n}{n!}(\rho-\kappa)^n. \tag{6.4}$$

Though, in general, κ is no special point for the function $h(\phi)$, it still enters in the definition of the vertex functions, from which one extracts the physical multimeson Yukawa couplings. As a consequence, in this regime it is necessary to change also the parametrizations of $h(\phi)$ and $y(\rho)$, as follows:

$$h(\phi) = \phi \sum_{n=0}^{N_h-1} \frac{h_n}{n!}(\rho-\kappa)^n \tag{6.5}$$

$$y(\rho) = \sum_{n=1}^{N_h} \frac{y_n}{n!}[(\rho-\kappa)^n - (-\kappa)^n]. \tag{6.6}$$

The pair (N_v, N_h), or more generally an ordering of the polynomial couplings by priority of inclusion in the truncations, can be chosen by relying on naive dimensional counting, as in an effective field theory setup, or on the knowledge of the dynamics at a deeper level, e.g. a global numerical solution for the FP functionals and the critical exponents. In the latter strategy, one would sort the critical exponents in order of relevance and would try to accurately describe the corresponding perturbations. Alternatively, and maybe less efficiently, one could scan over the results produced by different pairs (N_v, N_h) and select them on the base of a comparison to the global numerical solution. In the former strategy instead, since the dimension of a scalar self-interaction ϕ^{2n} is n and the one of a multimeson Yukawa coupling $\bar{\psi}\phi^{2n+1}\psi$ is $5/2+n$, we would expect that the pairs $(N_v = D, N_h = D-2)$, for the truncation of $h(\phi)$ given in Eqs. (6.2) and (6.5), correspond to including operators up to dimension D. However, since by truncating at level $N_h = D-2$ we loose information about an operator of dimension $D+1/2$, if we want to be slightly more accurate, we could include the latter and consider the pairs $(N_v = D, N_h = D-1)$. In our analysis we did perform to some extent a random scan over different pairs (N_v, N_h), and we found that the two strategies nicely agree, so that $(N_v = D, N_h = D-1)$ is a very good systematic choice for polynomial truncations. For similar reasons, as well as for the sake of comparison, we made the same choice also for the truncation of $y(\rho)$ given in Eqs. (6.3) and (6.6).

It is necessary to stress that, in both the parametrizations given above, even at lowest order in the truncation for the Yukawa coupling, the beta-functions for h_0 or y_1 are different from the classic result [27] illustrated in the reviews [34] and used for the present $d=3$ critical theory for instance in Refs. [14–16,18,19]. This happens because $\partial_t h(\phi)$, which comes from the projection of the rhs of the flow equation on the term $i\bar{\psi}\psi$, is a nonlinear function of ϕ, independent of the parametrization of $h(\phi)$, be it linear in ϕ or not. Hence, in order to define the running of a linear Yukawa coupling, a further projection is needed. The prescription adopted by the above-mentioned studies is to identify the beta-function of the linear Yukawa coupling with the first ϕ-derivative of $\partial_t h(\phi)$ at the minimum of the potential. For the truncations under consideration in this work instead, $\partial_t h_0$ comes from the zeroth-order ϕ-derivative of $\partial_t h(\phi)/\phi$, while $\partial_t y_1$ is defined as the first-order ρ-derivative of $\partial_t y(\rho) = 2h(\phi)\partial_t h(\phi)$, always evaluated at the minimum of the potential. Simplicity is our main motivation for choosing a parametrization of the running Yukawa sector which does not include the traditional Yukawa beta-function, as we are now going to explain.

The traditional projection has the structure of a Taylor expansion of $\partial_t h(\phi)$ about $\phi = \phi_0$ [ϕ_0 being the minimum of $v(\phi)$]. The choice of such an expansion for the parametrization of $h(\phi)$ would entail an explicit breaking of $\mathbb{Z}_2$ symmetry, which requires this function to be odd. Ideally, one would need to match two Taylor expansions, one about $\phi = \phi_0$ and another one about $\phi = -\phi_0$, by imposing suitable conditions at the origin. These are just provided by $\mathbb{Z}_2$ symmetry. The result of this construction, however, is not a simple Taylor expansion anymore,

$$h(\phi) = \frac{1}{2}\sum_{n=1}^{N_h}\frac{g_n}{n!}[(\phi-\phi_0)^n + (-1)^{n+1}(\phi+\phi_0)^n], \qquad (6.7)$$

and the projection rule on the generic coupling g_n is more involved than simply taking the nth ϕ-derivative and evaluating it at $\phi = \phi_0$. Yet it is true that the latter projection works for the N_hth coupling, such that this truncation does include the traditional beta-function of the linear Yukawa coupling as the $N_h = 1$ case. In this work we preferred to consider and compare only the two truncation schemes presented in Eqs. (6.2) and (6.5) and Eqs. (6.3) and (6.6), leaving the one in Eq. (6.7) aside. In the next sections, we are going to show that both polynomial truncations converge to the same results for large enough N_v and N_h, an observation that clearly should apply to all possible parametrizations. Furthermore, in both polynomial truncations, simply by setting $N_h = 1$, one gets estimates that are significantly different from the full truncation-independent results. That the latter statement also applies to the truncation in Eq. (6.7) can be assessed by comparison to the literature, which the reader can find in Sec. VI B.

A. LPA

In Sec. V we looked for the $d=3$ nontrivial critical theories at varying X_f within the LPA, by means of numerical solvers for the ODEs defining the FP potentials. Here we repeat this analysis with the different method of polynomial truncations, and we compare the results with the ones we previously found. The FPs emerge from the solution of a system of coupled nonlinear algebraic equations for the couplings. The critical exponents are defined by (minus) the eigenvalues of the stability matrix at the FP, i.e. the matrix of derivatives of the beta-functions with respect to the couplings [34]. The anomalous dimensions are computed in a non-self-consistent way, by neglecting them in the FP equations descending from Eqs. (2.3) and (2.4) and then by evaluating the flow equations for the wave function renormalizations Eqs. (2.5) and (2.6) at this FP position.

Let us start from the standard way of describing the Yukawa models, that is by approximating the Yukawa potential $h(\phi)$ with a single linear coupling. On the grounds of the results of the full functional analysis presented in Sec. V, one could expect that this approximation performs well, since far enough from the large-field region the FP function $h(\phi)$ does not strongly deviate from a straight line; see Fig. 4. For a linear Yukawa function, the expansions around the origin of $h(\phi)$ and $y(\rho)$ give results which are identical order by order in N_v, both in the shape of the FP functions (in the sense that $y_1 = 2h_0^2$ at the FP) and in the critical exponents. As a consequence we can present them in a single table for the former parametrization, the latter providing the same results. This is Table I, where we set e.g. $X_f = 1$. The first two critical exponents form a complex

TABLE I. Case $d = 3$ and $X_f = 1$, polynomial expansion of $h(\phi)$ around a trivial vacuum of the potential, with a fixed linear Yukawa function (standard Yukawa interaction), in the LPA.

(N_v, N_h)	(2,1)	(3,1)	(4,1)	(5,1)	(6,1)	(7,1)	(8,1)	(9,1)	(10,1)
λ_1	−0.04901	−0.1225	−0.1602	−0.1743	−0.1765	−0.1740	−0.1720	−0.1716	−0.1721
λ_2	5.887	6.841	7.128	7.204	7.214	7.203	7.193	7.191	7.193
λ_3	⋯	84.22	121.9	134.7	136.7	134.5	132.7	132.4	132.8
h_0	2.620	2.464	2.382	2.351	2.347	2.352	2.356	2.357	2.356
θ_1	1.701	1.546	1.438	1.378	1.358	1.362	1.372	1.376	1.375
θ_2	−1.050	−1.156	$-1.246 + i0.2686$	$-1.068 + i0.3386$	$-0.9602 + i0.3238$	$-0.9119 + i0.2933$	$-0.9150 + i0.2844$	$-0.9386 + i0.2941$	$-0.9526 + i0.3044$
θ_3	⋯	−1.864	$-1.246 - i0.2686$	$-1.068 - i0.3386$	$-0.9602 - i0.3238$	$-0.9119 - i0.2933$	$-0.9150 - i0.2844$	$-0.9386 - i0.2941$	$-0.9526 - i0.3044$
η_ψ	0.2395	0.2510	0.2572	0.2595	0.2599	0.2595	0.2591	0.2591	0.2592
η_ϕ	0.2620	0.2306	0.2150	0.2092	0.2083	0.2093	0.2101	0.2103	0.2101

conjugate pair, which is clearly unsatisfactory. This is produced by the expansion around a trivial minimum of $v(\phi)$, that for $X_f = 1$ is not justified. Once we turn to the SSB parametrization of $h(\phi)$, which is given on the top panel of Table II, they become real. However, things become cumbersome for the single-coupling SSB parametrization of $y(\rho)$, since we were not able to find any FP at all (which might nevertheless exist). Let us recall that, even in the case of a single Yukawa coupling, the beta-functions descending from the two different polynomial truncations of $h(\phi)$ and $y(\rho)$ are different, and hence one cannot simply translate the FP position from one parametrization to the other. As soon as we add y_2, the FP can be easily found. This then stimulates considering the general effect of allowing for higher polynomial Yukawa couplings.

TABLE II. Case $d = 3$ and $X_f = 1$, polynomial expansion of $h(\phi)$ around a nontrivial vacuum for both the potential and the Yukawa function, in the LPA, with or without the inclusion of multiple-meson-exchange interactions (top and bottom panels, respectively).

(N_v, N_h)	(5,1)	(6,1)	(7,1)	(8,1)	(9,1)
κ	0.01114	0.01115	0.01114	0.01114	0.01114
λ_2	25.08	24.88	24.80	24.84	24.85
λ_3	813.8	800.3	793.33	796.5	797.5
h_0	5.716	5.690	5.674	5.681	5.683
θ_1	1.338	1.333	1.336	1.336	1.335
θ_2	−0.2461	−0.2466	−0.2490	−0.2484	−0.2483
θ_3	−2.232	−2.060	−2.033	−2.067	−2.075
η_ψ	0.2629	0.2288	0.2288	0.2288	0.2288
η_ϕ	0.5259	0.5166	0.5155	0.5160	0.5162

(N_v, N_h)	(5,4)	(6,5)	(7,6)	(8,7)	(9,8)
κ	0.01002	0.01009	0.01008	0.01007	0.01007
λ_2	15.34	15.32	15.30	15.28	15.28
λ_3	508.3	506.8	503.6	502.1	502.1
h_0	4.220	4.211	4.207	4.206	4.207
h_1	48.23	47.73	47.46	47.43	47.48
θ_1	1.231	1.234	1.236	1.236	1.235
θ_2	−0.6144	−0.6078	−0.6080	−0.6106	−0.6117
θ_3	−1.649	−1.551	−1.520	−1.521	−1.531
η_ψ	0.3435	0.3409	0.3402	0.3404	0.3407
η_ϕ	0.4916	0.4910	0.4899	0.4895	0.4895

The immediate observation is that their inclusion significantly alters the position of the FP and the critical exponents. Some degree of convergence is observed in several systematic strategies for the increase of N_v and/or N_h, but this can be convergence to the wrong results, i.e. to FP functions that do not agree with the numerical global solution. The linear Yukawa truncations provide one example of this fact. This is visible by comparing the two panels of Table II, where on the rhs we show the results provided by the $(N_v = D, N_h = D - 1)$ systematic choice that we have already discussed above. The latter turns out to converge to the correct value of the FP couplings, as we are now going to argue. In Table III we show the results

TABLE III. Case $d = 3$ and $X_f = 1$, polynomial expansion of $y(\rho)$ in the LPA. Top panel: expansion around the origin, for which the global numerical solution provides $\lambda_1 = -0.1313$, $y_1 = 28.47$, and unstable higher couplings. Bottom panel: expansion around a nontrivial vacuum and, in the last column, the corresponding couplings extracted from the global numerical solution.

(N_v, N_h)	(4,3)	(5,4)	(6,5)	(8,7)	(9,8)
λ_1	−0.1209	−0.1315	−0.1339	−0.1315	−0.1309
λ_2	10.60	11.05	11.16	11.09	11.06
λ_3	293.2	339.6	351.0	342.7	340.1
y_1	26.84	28.38	28.76	28.53	28.44
y_2	986.6	1161	1206	1178	1167
θ_1	1.324	1.253	1.226	1.230	1.236
θ_2	−0.8293	−0.7186	−0.6410	−0.5892	−0.5989
θ_3	−2.690	−2.215	−1.838	−1.460	−1.446
η_ψ	0.5209	0.5615	0.5716	0.5642	0.5618
η_ϕ	0.4486	0.4645	0.4683	0.4663	0.4654

(N_v, N_h)	(5,4)	(6,5)	(7,6)	(8,7)	(9,8)	(∞, ∞)
κ	0.01000	0.01013	0.01006	0.01006	0.01007	0.01007
λ_2	15.58	15.17	15.30	15.28	15.28	15.28
λ_3	521.8	498.9	503.0	502.0	502.3	502.8
y_1	44.59	43.00	43.51	43.44	43.43	43.45
y_2	1925	1818	1842	1837	1837	1839
θ_1	1.260	1.221	1.236	1.236	1.235	1.228
θ_2	−0.6849	−0.7738	−0.5964	−0.6111	−0.6127	−0.624
θ_3	−1.693	−1.077	−1.511	−1.522	−1.537	−1.584
η_ψ	0.3458	0.3384	0.3410	0.3406	0.3406	⋯
η_ϕ	0.4955	0.4887	0.4897	0.4894	0.4895	⋯

obtained by the systematic $(D, D-1)$ extension of polynomial truncations for $y(\rho)$. Comparing the two panels, one can see how the critical exponents can be computed by large polynomial truncations independently of whether these are around the origin or a nontrivial vacuum. Furthermore, comparing the bottom panels of Tables III and II, it can be observed how both the FP potentials and the critical exponents converge to values that are independent of the chosen parametrization. That these values are the ones corresponding to the full global solution provided in Sec. V is shown in the bottom panel of Table III. Notice, however, that there is a 0.6% difference between the relevant exponent computed with the polynomial truncations and the one obtained by the global numerical analysis. Even if we feel that we have the former method under a better control, we cannot give our preference to any of these estimates.

In Fig. 9 we plot different kinds of polynomial solutions, all in a $(N_v = 9, N_h = 8)$ truncation, against the numerical global FP functions, still for $X_f = 1$. For the potential v, we show only the domain $\phi \geq 0.3$, the agreement among all the curves being perfect for smaller values. The expansion around the origin has a smaller domain of validity as expected. Regarding the two sets of expansions around a nontrivial vacuum, the scalar potentials for the two cases are almost indistinguishable, while for the Yukawa function, we obtain a slightly better result employing the one of Eq. (6.6), as it is shown in the right panel of the figure. The same kind of plots can be obtained for the polynomial truncations based on a single Yukawa coupling, corresponding to a linear Yukawa function. These are shown in Fig. 10, where we consider both polynomial expansions, around the origin and the nontrivial minimum, for $N_v = 9$. The left panel is especially interesting since it shows how, if

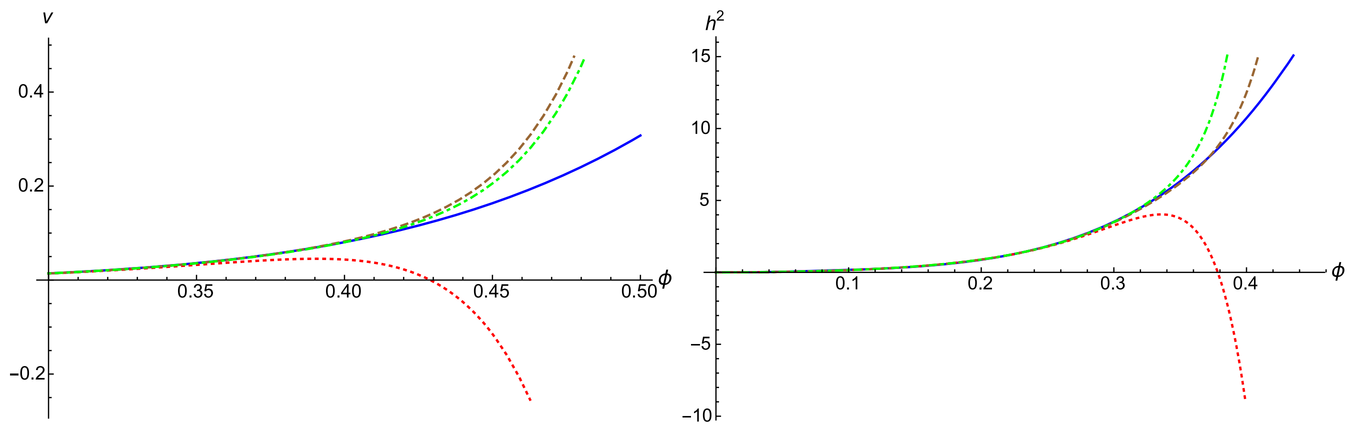

FIG. 9 (color online). Comparison of the $X_f = 1$ global numerical solution in the LPA (blue, continuous) with the corresponding $(N_v = 9, N_h = 8)$ polynomial solutions, around the origin as in Eqs. (6.1)–(6.3) (red, dotted), around a nontrivial vacuum as in Eqs. (6.4)–(6.6) (brown, dashed) and in Eqs. (6.4)–(6.5) (green, dot-dashed), for the potential $v(\phi)$ (left panel) and the Yukawa function $y(\phi) = h^2(\phi)$ (right panel).

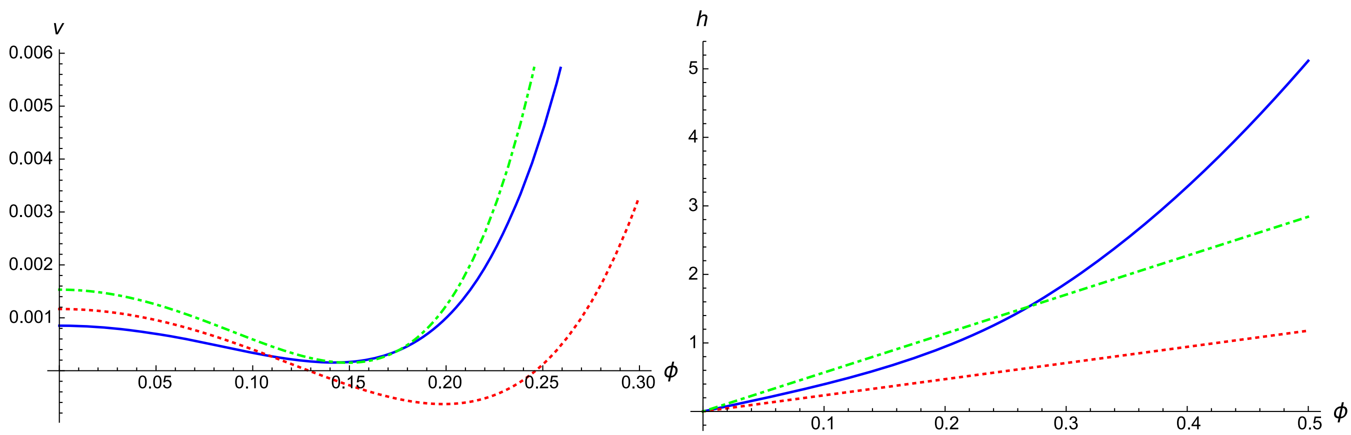

FIG. 10 (color online). Comparison of the $X_f = 1$ global numerical solution in the LPA (blue, continuous) with the corresponding $(N_v = 9, N_h = 1)$ polynomial solutions, around the origin as in Eqs. (6.1)–(6.3) (red, dotted) and around a nontrivial vacuum as in Eqs. (6.4) and (6.5) (green, dot-dashed), for the potential $v(\phi)$ (left panel) and the Yukawa function $h(\phi)$ (right panel).

TABLE IV. Case $d = 3$ and varying X_f, polynomial expansion of $h(\phi)$ around the nontrivial (top panel) or trivial (bottom panel) minimum for both the potential and the Yukawa function, with $N_h = 8$ and $N_v = 9$ in the LPA.

X_f	0.3	0.6	0.9	1.2	1.5	1.64
κ	2.311×10^{-2}	1.704×10^{-2}	1.173×10^{-2}	6.845×10^{-3}	2.219×10^{-3}	1.126×10^{-4}
λ_2	9.872	12.21	14.52	16.75	18.77	19.61
λ_3	183.6	294.3	443.4	632.5	856.0	967.6
h_0	4.154	4.178	4.200	4.218	4.227	4.230
h_1	35.08	40.29	45.66	51.12	56.52	59.04
θ_1	1.435	1.344	1.261	1.185	1.117	1.087
θ_2	−0.6683	−0.6481	−0.6216	−0.5896	−0.5466	−0.5212
θ_3	−1.022	−1.250	−1.464	−1.656	−1.887	−2.096
η_ψ	0.2780	0.3000	0.3292	0.3667	0.4164	0.4482
η_ϕ	0.2366	0.3111	0.4342	0.6249	0.8850	1.014

X_f	1.64	2	2.5	3	3.5
λ_1	-2.267×10^{-3}	0.1403	0.5480	1.705	6.165
λ_2	19.50	29.48	65.58	232.9	1698
λ_3	960.5	1955	7265	5.313×10^4	1.090×10^6
h_0	4.223	4.600	5.422	7.041	10.88
h_1	58.84	79.82	142.6	353.6	1505
θ_1	1.071	0.9976	0.9336	0.9538	1.041
θ_2	−0.5212	−0.4661	−0.3727	−0.2725	−0.1783
θ_3	−2.063	$-2.725 \pm i0.2953$	$-2.763 \pm i0.8557$	$-2.507 \pm i1.242$	$-1.956 \pm i1.695$
η_ψ	0.4521	0.3372	0.1066	−0.1522	−0.3048
η_ϕ	1.012	1.545	2.971	6.660	19.64

one forces a linear Yukawa function, even with the SSB expansion, the shape of the potential is poorly reproduced.

Having observed that in the LPA the $(D, D-1)$-systematic polynomial expansions converge to the global solution for $X_f = 1$, we assume that this is always the case and make use of them for addressing how the FP and the critical exponents depend on X_f within the LPA. In Sec. III we have argued that when X_f is not small there is no reason to trust the LPA for the $d = 3$ critical theory, since η_ϕ should approach unity as X_f increases. This is what the global numerical analysis also indicates. Indeed in Sec. V we found that the constants A and B wildly grow from $X_f = 3$ on, in practice making the construction of FP potentials harder and harder. This problem is easily addressed by means of the polynomial expansions. The results obtained with a (9,8) truncation, both for $h(\phi)$ and $y(\rho)$, are shown in Tables IV and V.

As expected, the anomalous dimensions show a very different X_f dependence. Starting with $\eta_\psi > \eta_\phi$ for very small X_f, the former decreases, and the latter increases as X_f is increased. Still for X_f around 1, the two are small enough for qualitatively trusting the LPA, though for estimates of the critical exponents, the LPA′ provides different and more accurate results. The polynomial truncations agree with the global analysis and locate around $X_f = 1.64$ the transition from the SSB to the SYM (symmetric) regime for the FP potential. Around this value η_ϕ reaches unity, thus signalling the inconsistent use of the LPA. Yet, if we insist on using this approximation for larger values of X_f, the breakdown of the approach is signalled by different phenomena. First of all the critical exponents become complex, from about $X_f = 2$ on. Then the anomalous dimensions η_ϕ and η_ψ, which are determined in a somehow unlegitimate way, become much bigger than unity and negative, respectively. At the same time, the couplings at the FP increase very rapidly, similarly to what was observed in Fig. 5. Actually in LPA it is easier than in the global numerical analysis to understand how quickly they grow. The result of a (6,5)-polynomial truncation of $y(\rho)$ around a trivial minimum is shown in Fig. 11. It is quite accurate to fit the behavior of the coupling y_1 close to $X_f = 4$ with a simple pole $y_1 \approx 121.2/(3.999 - X_f)$. Also the remaining couplings have a rate of growth that is compatible to a divergence at a finite value of X_f, but these values would lie beyond the pole of y_1.

Also the comparison between the polynomial truncations and the global numerical results illustrates the appearance of severe problems as X_f increases. Moving to larger values of X_f and entering the symmetric regime, one sees, again comparing against the numerical solution of the ODEs, that the polynomial approximation has a smaller radius of convergence and therefore leads to a less trustworthy estimate of the LPA results. As an example we present the case $X_f = 2.5$ in Fig. 12. Here the two curves show a

TABLE V. Case $d = 3$ and varying X_f, polynomial expansion of $y(\rho)$ around the nontrivial (top panel) or trivial (bottom panel) minimum for both the potential and the Yukawa function, with $N_h = 8$ and $N_v = 9$ in the LPA.

X_f	0.3	0.6	0.9	1.2	1.5	1.64
κ	2.310×10^{-2}	1.705×10^{-2}	1.174×10^{-2}	6.846×10^{-3}	2.187×10^{-3}	3.115×10^{-5}
λ_2	9.889	12.21	14.52	16.75	18.75	19.56
λ_3	184.1	294.1	443.4	632.6	853.3	961.5
y_1	48.27	46.33	44.26	41.48	37.82	35.78
y_2	1413	1600	1783	1927	1997	1997
θ_1	1.436	1.344	1.261	1.184	1.112	1.077
θ_2	−0.6818	−0.6643	−0.6245	−0.5897	−0.5459	−0.7877
θ_3	−1.021	−1.242	−1.467	−1.665	−1.864	−0.5190
η_ψ	0.2789	0.2998	0.3290	0.3667	0.4171	0.4498
η_ϕ	0.2367	0.3111	0.4342	0.6249	0.8850	1.014

X_f	1.64	2	2.5	3	3.5
λ_1	-6.085×10^{-4}	0.1424	0.5501	1.706	6.164
λ_2	19.53	29.52	65.65	232.8	1698
λ_3	959.5	1954	7258	5.301×10^4	1.089×10^6
y_1	35.72	42.37	58.84	99.13	236.9
y_2	1993	2944	6192	1.990×10^4	1.310×10^5
θ_1	1.076	1.003	0.9374	0.9551	1.041
θ_2	−0.5196	−0.4652	−0.3727	−0.2726	−0.1783
θ_3	−2.006	−2.582	$-2.794 \pm i0.8023$	$-2.520 \pm i1.231$	$-1.958 \pm i1.694$
η_ψ	0.4509	0.3360	0.1061	−0.1520	−0.3048
η_ϕ	1.014	1.548	2.974	6.659	19.64

good overlap for $\phi < 0.18$, both for $v(\phi)$ and $y(\phi)$, while at $X_f = 1$ the same grade of agreement was found for $\phi < 0.28$. Again the strongest restriction is imposed by the Yukawa function. Instead of interpreting these problems as a sign of the generic weakness of the polynomial truncations for large X_f, we take the point of view that they are the way in which these truncations manifest the failure of the LPA for X_f roughly bigger than 1.6. We think that the results of the next section support this interpretation.

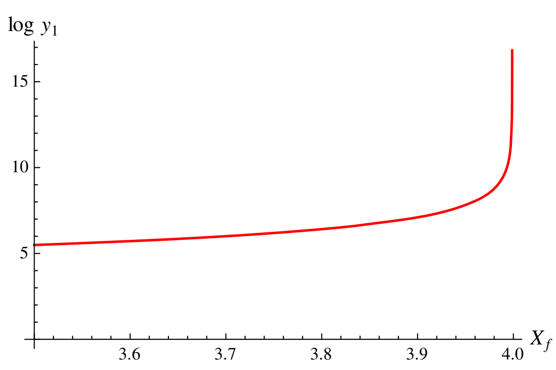

FIG. 11 (color online). Behavior of the coupling y_1 in a $N_h = 5$, $N_v = 6$ polynomial truncation of $y(\rho)$ around a trivial vacuum, within the LPA. The curve is a fit of data from $X_f = 3.5$ to $X_f = 4–10^{-7}$.

B. LPA′

In the LPA′ the anomalous dimensions are consistently determined by solving the FP equations together with the flow equations for the wave function renormalizations. In the previous sections, we have shown that this is necessary for a correct qualitative description of the dynamics of the model, roughly above $X_f \approx 1.6$. The expectation is that, thanks to the wave function renormalizations, the system should gradually move toward the large-X_f limit, as it was already checked for truncations with a linear Yukawa function [14–17]. In this section we want also to understand how big are the effects of the wave function renormalizations on the critical exponents, already for small X_f.

As in the previous section, let us start our discussion with the $X_f = 1$ model. Table VI is the LPA′ version of Table II, which considers the truncation of $h(\phi)$ with or without higher Yukawa couplings. If the effect of the inclusion of multimeson exchange on the relevant exponent θ_1 was of the 8% in the LPA, it got reduced to the 7% in the LPA′. However, in the truncation of $y(\rho)$, the effect is of the 20%, see Table VII. Also, the convergence of the polynomial truncations seems quicker in the LPA′. A comparison between the top panels of Tables VI and VII illustrates how the predictions of the FRG can be made independent of the truncation scheme, here in the form of a different definition of Yukawa couplings, only by including full

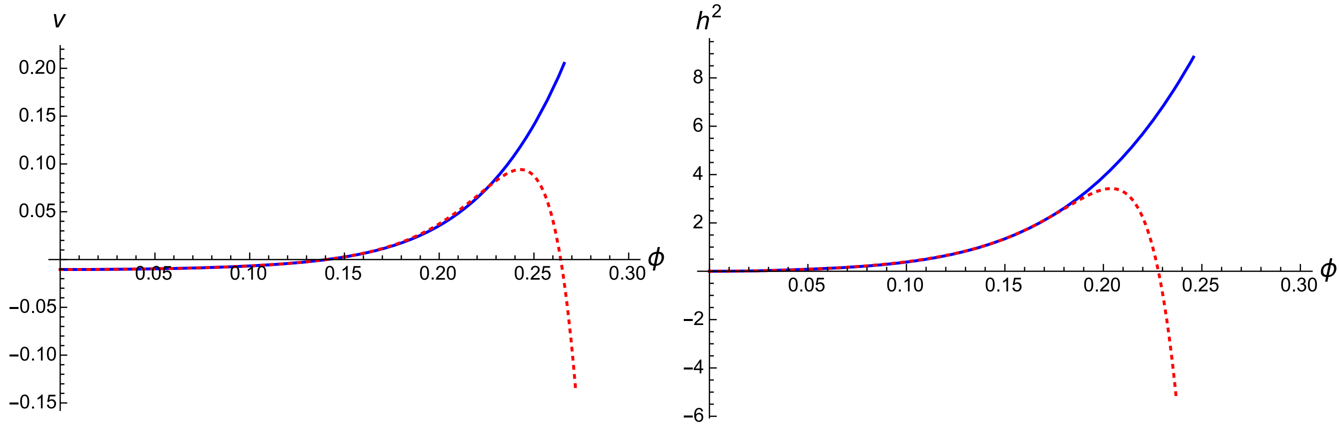

FIG. 12 (color online). Comparison of the numerical solution in the LPA (blue, continuous) with the corresponding $(N_v = 9, N_h = 8)$-polynomial solutions, for $X_f = 2$, around the origin as in Eqs. (6.1)–(6.3) (red, dotted), around a nontrivial vacuum as in Eqs. (6.4)–(6.6) (brown, dashed), and in Eqs. (6.4) and (6.5) (green, dot-dashed), for the potential v (left panel) and the Yukawa function $y(\phi) = h^2(\phi)$ (right panel).

functions of field amplitudes, that is by allowing for higher polynomial couplings.

Once we turn to the dependence of the results on X_f, which is shown in Tables VIII and IX, it becomes visible how the difference between the LPA and the LPA′ can be negligible only for unphysical very small values of X_f. For θ_1, it is the 7% at $X_f = 0.3$ and the 14% already at $X_f = 1$.

TABLE VI. Case $d = 3$ and $X_f = 1$, polynomial expansion of $h(\phi)$ around a nontrivial vacuum for both the potential and the Yukawa function, in the LPA′, with or without the inclusion of multiple-meson-exchange interactions (bottom and top panels, respectively).

(N_v, N_h)	(5,1)	(6,1)	(7,1)	(8,1)	(9,1)
κ	6.250×10^{-3}	0.01261	0.01262	0.01262	0.01262
λ_2	6.299	6.995	7.000	7.001	7.000
λ_3	52.38	64.06	64.28	64.33	64.29
h_0	2.139	2.533	2.534	2.534	2.534
θ_1	1.595	1.548	1.548	1.548	1.548
θ_2	−0.7528	−0.6828	−0.6832	−0.6828	−0.6828
θ_3	−1.241	−1.289	−1.299	−1.297	−1.294
η_ψ	0.1168	0.1273	0.1272	0.1272	0.1272
η_ϕ	0.2807	0.2237	0.2238	0.2238	0.2238

(N_v, N_h)	(5,4)	(6,5)	(7,6)	(8,7)	(9,8)
κ	0.01080	0.01078	0.01077	0.01078	0.01078
λ_2	6.009	5.998	5.997	5.998	5.999
λ_3	61.01	60.50	60.47	60.54	60.56
h_0	2.474	2.473	2.474	2.474	2.474
h_1	7.548	7.530	7.542	7.545	7.544
θ_1	1.444	1.443	1.443	1.443	1.443
θ_2	−0.7721	−0.7739	−0.7745	−0.7743	−0.7741
θ_3	−1.078	−1.077	−1.084	−1.086	−1.085
η_ψ	0.1535	0.1535	0.1536	0.1536	0.1536
η_ϕ	0.2214	0.2211	0.2211	0.2212	0.2212

On the contrary, as we will see later in this section by comparing our results to the literature, the effect of the inclusion of higher Yukawa couplings decreases with increasing X_f. The transition between the SSB and the symmetric regime for the FP potential in the LPA′ is around $X_f = 1.62$, while it occurs at $X_f = 2.31$ for truncations with a linear Yukawa function [19]. From these tables it also seems reasonable to expect that in the $X_f \to 0$ limit the Yukawa couplings attain finite nonvanishing values, as it was observed already in the LPA; see Fig. 6. Also, the trend in the change of θ_1 and η_ϕ is compatible with an approach to the corresponding Ising values, thus further supporting the discussion at the end of Sec. II. As far as the $X_f \to \infty$ limit is concerned instead, the smooth transition to the large-X_f exponents is evident in the bottom panels of Tables VIII and IX.

Let us now come to the comparison of our results with the literature. The classic methods for the investigation of the critical properties of the Gross–Neveu and Yukawa models are the ϵ and the $1/N_f$ expansions [2–8]. The former can be of great utility, since both expansions around the upper and the lower critical dimensions give comparable results, such that $d = 3$ does not seem a too wild extrapolation. Yet, some treatment for these asymptotic series is needed. Resummation is unfortunately out of reach, since they are known only up to the second or third orders [3,5], apart for the anomalous dimensions for which the computations have been pushed up to the fourth order [6]. Polynomial interpolations of the two different ϵ expansions have been studied in Ref. [18] for the case $X_f = 8$, and we report their results, borrowing their notations, such that $P_{i,j}$ denotes a polynomial which is i-loop exact near the lower critical dimension and j-loop exact near the upper. We also report the crude extrapolations that are obtained by simply setting $\epsilon = 1$ in the

TABLE VII. Case $d = 3$ and $X_f = 1$, polynomial expansion of $y(\rho)$ around a nontrivial vacuum for both the potential and the Yukawa function, in the LPA′, with or without the inclusion of multiple-meson-exchange interactions (bottom and top panels, respectively).

(N_v, N_h)	(5,1)	(6,1)	(7,1)	(8,1)	(9,1)
κ	9.208×10^{-3}	9.210×10^{-3}	9.212×10^{-3}	9.213×10^{-3}	9.212×10^{-3}
λ_2	8.300	8.307	8.315	8.316	8.314
λ_3	72.23	72.45	72.77	72.82	72.71
y_1	18.64	18.65	18.67	18.67	18.67
θ_1	1.732	1.731	1.732	1.732	1.732
θ_2	−0.5319	−0.5324	−0.5325	−0.5318	−0.5321
θ_3	−1.626	−1.657	−1.676	−1.672	−1.664
η_ψ	0.1886	0.1887	0.1887	0.1887	0.1887
η_ϕ	0.2680	0.2681	0.2683	0.2684	0.2683
(N_v, N_h)	(5,4)	(6,5)	(7,6)	(8,7)	(9,8)
κ	0.01079	0.01077	0.01078	0.01078	0.01078
λ_2	6.005	5.997	5.997	5.999	5.999
λ_3	60.83	60.43	60.50	60.59	60.56
y_1	13.05	13.04	13.04	13.04	13.04
y_2	152.0	151.4	151.7	151.8	151.7
θ_1	1.444	1.443	1.443	1.443	1.443
θ_2	−0.7710	−0.7738	−0.7745	−0.7743	−0.7741
θ_3	−1.072	−1.077	−1.086	−1.086	−1.084
η_ψ	0.1536	0.1536	0.1536	0.1536	0.1536
η_ϕ	0.2214	0.2211	0.2211	0.2212	0.2212

TABLE VIII. Case $d = 3$ and various X_f, polynomial expansion of $h(\phi)$ around the nontrivial (top panel) or trivial (bottom panel) minimum for both the potential and the Yukawa function, with $N_h = 8$ and $N_v = 9$ in the LPA′.

X_f	0.3	0.6	0.9	1.2	1.5	1.62
κ	2.377×10^{-2}	1.793×10^{-2}	1.253×10^{-2}	7.316×10^{-3}	2.171×10^{-3}	1.164×10^{-4}
λ_2	5.719	6.028	6.045	5.849	5.530	5.385
λ_3	55.00	61.19	61.55	57.38	50.81	47.92
h_0	2.745	2.641	2.518	2.385	2.252	2.201
h_1	9.355	8.798	7.890	6.831	5.789	5.400
θ_1	1.537	1.490	1.453	1.427	1.411	1.407
θ_2	−0.8158	−0.7883	−0.7755	−0.7751	−0.7833	−0.7879
θ_3	−0.9829	−1.066	−1.089	−1.063	−1.004	−0.9742
η_ψ	0.1510	0.1529	0.1537	0.1531	0.1514	0.1505
η_ϕ	0.1366	0.1687	0.2073	0.2499	0.2936	0.3108
X_f	1.62	2	3	4	6	8
λ_1	-7.622×10^{-4}	4.135×10^{-2}	0.1443	0.2316	0.3602	0.4448
λ_2	5.375	5.472	5.604	5.562	5.185	4.701
λ_3	47.83	43.65	32.95	23.64	11.05	4.560
h_0	2.198	2.157	2.037	1.915	1.703	1.538
h_1	5.388	4.863	3.635	2.694	1.537	0.9481
θ_1	1.277	1.229	1.134	1.077	1.024	1.004
θ_2	−0.7776	−0.7742	−0.7794	−0.7962	−0.8345	−0.8649
θ_3	−0.8944	−0.9581	−1.101	−1.196	−1.287	−1.311
η_ψ	0.1508	0.1314	9.347×10^{-2}	6.939×10^{-2}	4.341×10^{-2}	3.073×10^{-2}
η_ϕ	0.3106	0.3721	0.5057	0.6024	0.7223	0.7894

TABLE IX. Case $d = 3$ and various X_f, polynomial expansion of $y(\rho)$ around the nontrivial (top panel) or trivial (bottom panel) minimum for both the potential and the Yukawa function, with $N_h = 8$ and $N_v = 9$ in the LPA′.

X_f	0.3	0.6	0.9	1.2	1.5	1.62
κ	2.377×10^{-2}	1.793×10^{-2}	1.253×10^{-2}	7.315×10^{-3}	2.169×10^{-3}	1.125×10^{-4}
λ_2	5.719	6.028	6.045	5.849	5.530	5.384
λ_3	55.00	61.19	61.55	57.37	50.79	47.90
y_1	17.51	15.62	13.67	11.85	10.26	9.690
y_2	214.7	192.0	162.1	131.55	104.5	95.07
θ_1	1.537	1.490	1.453	1.427	1.411	1.407
θ_2	−0.8152	−0.7882	−0.7755	−0.7751	−0.7831	−0.7877
θ_3	−0.9833	−1.066	−1.088	−1.062	−1.003	−0.9727
η_ψ	0.1510	0.1529	0.1537	0.1531	0.1514	0.1505
η_ϕ	0.1366	0.1687	0.2073	0.2499	0.2936	0.3108

X_f	1.62	2	3	4	6	8
λ_1	-7.366×10^{-4}	4.137×10^{-2}	0.1443	0.2316	0.3602	0.4448
λ_2	5.374	5.471	5.604	5.562	5.185	4.701
λ_3	47.81	43.63	32.95	23.64	11.05	4.560
y_1	9.667	9.304	8.296	7.338	5.804	4.733
y_2	94.77	83.91	59.23	41.28	20.95	11.67
θ_1	1.277	1.229	1.134	1.077	1.024	1.004
θ_2	−0.7775	−0.7742	−0.7794	−0.7962	−0.8345	−0.8649
θ_3	−0.8935	−0.9578	−1.101	−1.196	−1.287	−1.311
η_ψ	0.1508	0.1314	9.347×10^{-2}	6.939×10^{-2}	4.341×10^{-2}	3.073×10^{-2}
η_ϕ	0.3106	0.3721	0.5057	0.6024	0.7223	0.7894

expansions of $\theta_1 = \nu^{-1}$, η_ϕ, and η_ψ.[1] Also the $1/N_f$ expansion clearly needs some care, since we are interested in a low number of fermions. Actually we are going to refer to this method only for $X_f = 8$ and $X_f = 4$, corresponding to $N_f = 2$ and $N_f = 1$, respectively. Again only the second or third order is known [7,8]. For the correlation-length exponent $\theta_1 = \nu^{-1}$, we adopt the Padé approximant used in Ref. [18], while for the anomalous dimensions, we refer to the Padé–Borel treatment reported in Ref. [15].

The available FRG literature is rich, and it offers a precious background on which we can measure the effects of the enlargement of the truncation discussed in this work. Essentially all the past studies considered the LPA′, including a scalar potential and a simple linear Yukawa coupling [14–19], that can be considered as the first order in the truncation of Eq. (6.7). The only exception in this sense is provided by the supersymmetry-preserving scheme that has been applied to the $X_f = 1$ case, which retained a full superpotential [42–44], thus including multimeson exchange in the Yukawa sector, and sometimes was pushed to the next-to-next-to-leading order of the (supercovariant) derivative expansion. Also the choice of regulators is diverse, comprehending the linear, the sharp, and the exponential ones (which in the tables we abbreviate with lin, sha, and exp). In some studies the scalar potential was approximated by polynomial truncations in the symmetric regime, for which we provide the corresponding N_v (N_w in case of truncations of the superpotential for supersymmetric flows). In others, that we label by $N_v = \infty$ (or $N_w = \infty$), the differential equations for the FP and the perturbations around it were solved by numerical methods, which are different from paper to paper. Our results are labeled by $N_h > 1$.

Other methods to which we can compare in special cases are Monte Carlo simulations and the conformal bootstrap. Both of them can give high-precision computations of the critical exponents, but so far they have had a limited application to low-X_f Yukawa models. For $X_f = 8$ two lattice calculations of the critical exponents are available. One, based on staggered fermions [10], though ignoring a sign problem, provides results which are in good agreement with continuum methods, as it appears from Table X. An independent work applying the fermion bag approach [12], that is free from the sign problem, is instead offering very different results: $\nu = 0.83(1)$, $\eta_\phi = 0.62(1)$, and $\eta_\psi = 0.38(1)$. In both cases it is not clear whether the symmetry of the lattice model is the expected one in the continuum limit.[2] Recently, another sign-problem-free simulation adopting the continuous time quantum Monte Carlo method for a model of spinless fermions on a honeycomb lattice

[1]We made use of the formulas reported in Ref. [3], with typos corrected according to the observations of Ref. [18].

[2]We are grateful to H. Gies for informing us about these discussions.

TABLE X. Critical exponents for $X_f = 8$. For a short description of the approximations involved in each method, see the main text.

	ν	θ_1	η_ϕ	η_ψ
FRG $(N_v = 9, N_h = 8)$ lin (this work)	1.004	0.996	0.789	0.031
FRG $(N_v = 3, N_h = 1)$ exp [15]	1.016	0.984	0.786	0.028
FRG $(N_v = 6, N_h = 1)$ sha [18]	1.022	0.978	0.767	0.033
FRG $(N_v = 11, N_h = 1)$ lin [16]	1.018	0.982	0.760	0.032
FRG $(N_v = \infty, N_h = 1)$ lin [15]	1.018	0.982	0.756	0.032
FRG $(N_v = \infty, N_h = 1)$ lin [19]	1.018	0.982	0.760	0.032
Monte-Carlo [10]	1.00(4)	1.00(4)	0.754(8)	...
$1/N_f$ 2nd/3rd order [8,18]	1.040	0.962	0.776	0.044
$(2+\epsilon)$ 3rd order [5]	1.309	0.764	0.602	0.081
$(4-\epsilon)$ 2nd order [3]	0.948	1.055	0.695	0.065
$P_{2,2}$ interpolated ϵ-expansion [18]	1.005	0.995	0.753	0.034
$P_{3,2}$ interpolated ϵ-expansion [18]	1.054	0.949	0.716	0.041

TABLE XI. Critical exponents for $X_f = 4$. For a short description of the approximations involved in each method, see the main text.

	ν	θ_1	η_ϕ	η_ψ
FRG $(N_v = 9, N_h = 8)$ lin (this work)	0.929	1.077	0.602	0.069
FRG $(N_v = 3, N_h = 1)$ exp [15]	0.962	1.040	0.554	0.067
FRG $(N_v = \infty, N_h = 1)$ lin [15,19]	0.927	1.079	0.525	0.071
Monte-Carlo [13]	0.80(3)	1.25(3)	0.302(7)	...
$1/N_f$ 2nd/3rd order [7,8,18]	0.955	1.361	0.635	0.105
$(4-\epsilon)$ 2nd order [3]	0.862	1.160	0.502	0.110

TABLE XII. Critical exponents for $X_f = 2$. For a short description of the approximations involved in each method, see the main text.

	ν	θ_1	η_ϕ	η_ψ
FRG $(N_v = 9, N_h = 8)$ lin (this work)	0.814	1.229	0.372	0.131
FRG $(N_v = 3, N_h = 1)$ exp [15]	0.633	1.580	0.319	0.113
FRG $(N_v = 3, N_h = 1)$ lin [15]	0.623	1.605	0.308	0.112
FRG $(N_v = \infty, N_h = 1)$ exp [15]	0.640	1.563	0.319	0.114
FRG $(N_v = \infty, N_h = 1)$ lin [15]	0.621	1.610	0.308	0.112
FRG $(N_v = \infty, N_h = 1)$ lin [19]	0.4836	2.068	0.3227	0.1204
$(4-\epsilon)$ 2nd order [3]	0.773	1.293	0.317	0.154

provided estimates of the critical exponents of the chiral Ising universality class for $X_f = 4$, i.e. a single Dirac field [13]. These results are compared to those emerging from the continuum methods in Table XI. Surprisingly they are much closer to our estimates for the case $X_f = 2$; see Table XII.

Regarding the latter case, notice that the results from Ref. [15] are affected by the absence of some terms in the flow equations that, being proportional to the vacuum expectation value of the scalar, become important for $X_f \leq 2$.[3] Their effect significantly reduces the value of ν. Since upon inclusion of multimeson exchange the transition from the symmetric to the SSB regime occurs at lower values of X_f, our computations are still in the symmetric regime. This might qualitatively explain the drastic departure from the results of Ref. [19].

Also the comparison for $X_f = 1$, which is presented in Table XIII, requires some comments. Let us recall that for this field content the system at criticality is described by a $\mathcal{N} = 1$ Wess–Zumino model [17,24]. Hence, if the regularization does not break supersymmetry, the critical anomalous dimensions of the scalar and of the spinor should be equal. Furthermore, a superscaling relation $\nu^{-1} = (d - \eta)/2$, which was first

[3] See the discussion in Ref. [19].

TABLE XIII. Critical exponents for $X_f = 1$. About the FRG results, the schemes, the regulators, and the approximations being very different, see the main text.

	ν	θ_1	θ_2	η_ϕ	η_ψ	3-2θ_1
FRG ($N_v = 9, N_h = 8$) lin (this work)	0.693	1.443	−0.796	0.154	0.221	0.114
SUSY FRG ($N_w = \infty$) opt $n = 2$ NLO [43]	0.711	1.407	−0.771	0.186	0.186	0.186
SUSY FRG ($N_w = \infty$) opt $n = 2$ NNLO [43]	0.710	1.410	−0.715	0.180	0.180	0.180
SUSY FRG ($N_w = \infty$) opt $n = 1$ [44]	0.708	1.413	−0.381	0.174	0.174	0.174
SUSY FRG ($N_w = \infty$) opt $n = 2$ [44]	0.706	1.417	−0.377	0.167	0.167	0.167
FRG ($N_v = 2, N_h = 1$) 1-loop [17]	0.72	1.39	−0.71	0.15	0.15	0.22
$(4-\epsilon)$ 1st order [24]	⋯	⋯	⋯	0.143	0.143	⋯
$(4-\epsilon)$ 2nd order [3]	0.710	1.408	⋯	0.184	0.184	0.184
Conformal Bootstrap [46]	⋯	⋯	⋯	0.13	0.13	⋯

observed in Ref. [45] and later proved to hold at any order in the supercovariant derivative expansion in Ref. [43], is expected to hold. This is what happens for example in the ϵ expansions or in the supersymmetry-preserving FRG (SUSY FRG). Since the scheme adopted in the present work explicitly breaks supersymmetry, we expect and observe violations of these properties. Also in Ref. [17] supersymmetry is broken by regularization, and these violations are present, but they could be partially reduced or canceled by tuning the regulator. This tuning gives the results reported in Table XIII. A similar analysis of the regulator dependence of universal quantities and of the consequent breaking of supersymmetry could be performed in future studies for the present family of truncations. Yet, even by explicitly breaking the FP supersymmetry, we get exponents which are not very far from the ones produced by the above-mentioned methods. Let us add few details on the SUSY FRG results shown in Table XIII. They are obtained by setting one of the regulators to zero and choosing a shape similar to the linear regulator for the other, with an exponent n that differentiates between the conventional linear regulator (opt $n = 2$) and a slight variant (opt $n = 1$). Also the truncation scheme is different from the one discussed in the present paper, since it is related to an expansion in powers of the supercovariant derivative, that has been considered at the level of the LPA′ [42,44], at next-to-leading order (NLO) or at next-to-next-to-leading order (NNLO) [43]. For the case $X_f = 1$, we can also compare with a pioneering study based on the conformal bootstrap [46]. In Table XIII we included the one-loop computations of Refs. [17,24], even if two-loop results are on the market [3], on the basis of the naive observation that for Yukawa systems with complex scalars and spinors, the FP of which should effectively show $\mathcal{N} = 2$ supersymmetry [25], the anomalous dimensions obtained from the first order of the $(4-\epsilon)$ expansion, $\eta_\phi = \eta_\psi = 1/3$, agree with the available exact results [47].

VII. d=4

From the leading order of the $1/X_f$ expansion, one expects that for large enough X_f the chiral Ising FP merges with the Gaussian FP in the $d \to 4$ limit. Also at $X_f = 0$, for which we know from the discussion at the end of Sec. II that only mirrored images of the purely scalar FPs can exist, one can observe that the latter merge with the Gaussian FP for $d \to 4$, compatibly with the presumed triviality of four-dimensional scalar theory. This is illustrated in Fig. 13, which is produced as Fig. 3 but integrates only the FP equation for $h(\phi)$ at $v(\phi) = 0$ and $X_f = 0$ in the LPA′. Yet it remains to be shown what happens for a small nonvanishing number of fermions. Dimensional analysis indicates $d = 4$ as the upper critical dimension for any X_f. This can be checked by means of the FRG, either by numerical integration of the FP equation, as it was shown for example in Sec. IV for $X_f = 1$, or by the polynomial truncations discussed in the last sections. Indeed, the latter have already been used in the past, precisely to address this question.

In fact, an exploratory study of what happens to the $d \to 4$ limit in a $\mathbb{Z}_2$-symmetric Yukawa model with very

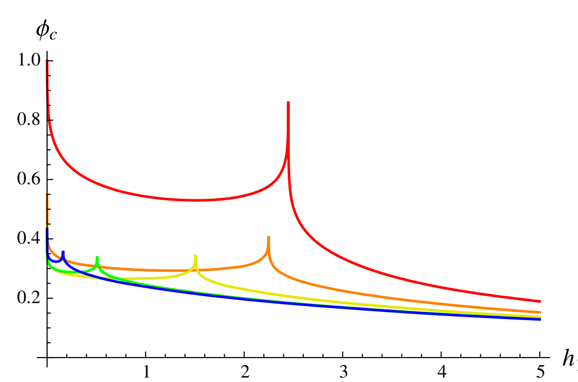

FIG. 13 (color online). Spike plots for $X_f = 0$, $v(\phi) = 0$, and $d \in \{3.5, 3.7, 3.9, 3.99, 3.999\}$ from red (upper) to blue (lower) in the LPA′.

small X_f was performed in Ref. [28], in order to test a mechanism for the generation of nontrivial FPs in fermion-boson models, that has subsequently found in chiral-Yukawa models some natural candidates [29]. That analysis pointed out that, within a $(N_v = 2, N_h = 1)$ polynomial truncation, according to the scheme of Eq. (6.7), the FRG detects nontrivial FPs also in $d = 4$, for unphysical small values of X_f. This holds both in the LPA and in the LPA′. However, the fact that the FP position and the critical exponents are significantly different in the two approximations was interpreted as a signal of the need to include further boson-fermion interactions in the truncation, in order to understand if these FPs are physical or merely an artifact of the approximations. This section reports on the changes brought by the different treatment of the Yukawa sector presented in this work.

At the level of the LPA, we generated three-dimensional plots similar to the ones illustrated in Fig. 1, second panel, by shooting from the origin with random values of $(v''(0), h'(0))$, for several values of $X_f < 1$, and we looked for spikes signalling possible FPs, but we have not found any of them. We were also not able to produce any global solution studying numerically the Cauchy problem from the asymptotic region, along the lines of Sec. V. We then reconsidered the analysis at the level of polynomial truncations. Already trying to reproduce the results of Ref. [28] in other truncations with $N_v = 2$ and $N_h = 1$ can be a nontrivial test, because of the different beta-function of the Yukawa coupling, associated to different projection rules. We have already argued that a change of the results depending on the parametrization employed signals the presence of errors induced by the use of inconsistent truncations. We first concentrated on the LPA, which at least for $d < 4$ is able to reproduce the right number of nontrivial FPs. In this case, the truncation adopted in Ref. [28] allows for non-Gaussian FPs approximately for $X_f \leq 1$. For instance, at $X_f = 0.4$ one can find the FP

$$\kappa = 0.00165, \qquad \lambda_2 = 27.26, \qquad g_1^2 = 81.13 \tag{7.1}$$

with two relevant directions

$$\theta_1 = 2.372, \qquad \theta_2 = 0.592, \qquad \theta_3 = -2.859. \tag{7.2}$$

We observed that in a polynomial truncation of $y(\rho)$ as in Eq. (6.6) the FP position is different,

$$\kappa = 0.00167, \qquad \lambda_2 = 54.18, \qquad y_1 = 494.0, \tag{7.3}$$

as well as the critical exponents,

$$\theta_1 = 1.653, \qquad \theta_2 = 0.932, \qquad \theta_3 = -3.445. \tag{7.4}$$

Still, the changes are not dramatic. On the other hand, we could not find any real FP within the same order of the truncation of $h(\phi)$ given in Eq. (6.5). We tried to circumvent this problem as in $d = 3$, by following the FP found in one parametrization to higher orders and then translating back to the other parametrization. Yet we were not able to reveal the FP for $y(\rho)$ for bigger values of N_v and N_h nor find it by chance in different orders of the truncation of $h(\phi)$.

Hoping that the inclusion of the wave function renormalizations could stabilize the polynomial truncations and help us in the search for FPs, we then considered LPA′, using the results of Ref. [28] as a guide for the localization of the interesting region in the space of couplings. While the FP is present in the first order of the truncation of Eq. (6.7), we could not find it in the parametrizations considered in this paper. Let us once more stress that this does not completely exclude that it can be found by other methods, even if we consider this very unlikely. Nevertheless, for the LPA′ we have not tried a numerical shooting at nonvanishing X_f as in the LPA. Hence, a more careful numerical analysis is needed, to exclude with a higher level of confidence the presence of low-X_f FPs in the theory space described by the truncation in Eq. (2.2). An even better test would be to consider the full next-to-leading order of the derivative expansion.

VIII. CONCLUSIONS

A proper quantitative control of the quantum dynamics of the $\mathbb{Z}_2$-symmetric Yukawa model, beyond the domain of applicability of perturbative methods, is important not only from a generic field-theoretical point of view but also for phenomenological reasons, since the latter is very useful as a toy model of numerous condensed matter systems, as well as of specific sectors of modern particle theory; see Sec. I for more details. The functional renormalization group is a simple analytic nonperturbative method that can provide a detailed description of strongly coupled systems, under approximations that are testable and improvable in several systematic ways. Furthermore, these results can be produced, almost simultaneously, in a continuous number of spacetime dimensions d and fermionic degrees of freedom X_f, thus allowing for a quick analysis of the dependence of the dynamics on the latter parameters.

In this work we focused on the critical behavior of the $\mathbb{Z}_2$-symmetric Yukawa model at zero temperature and density. Our principal aim was to test the impact of multimeson exchange, encoded in a Yukawa coupling which is a full function of the scalar field, on the FRG description of the latter behavior, a question that to our knowledge has never been considered before. Nevertheless, our analysis is relevant not only for the FRG community. For instance, in Sec. III we discussed the leading order of the $1/X_f$ expansion, the results of which can be directly exported out of the FRG framework in which we produced them and recovered also by different methods. This study illustrated how, by allowing for multimeson exchange, one can describe the generation of multicritical conformal Yukawa models as d is lowered from $d = 3$ toward $d = 2$, across the corresponding upper critical dimensions $d_n = 2 + 2/n$, with n a positive integer. We also showed how the large-X_f limit quantizes the corresponding critical anomalous dimension $\eta_\phi = d_n - d$. In Sec. IV we checked that this pattern of generation of critical theories as a function of d holds also at $X_f = 1$, and presumably at any other finite X_f. This would imply that in the $d \to 4$ limit only the Gaussian fixed point survives. The latter statement, being of special relevance for particle physics, was further analyzed in Sec. VII, where we argued that it applies also for $X_f < 1$, at least within the Ansatz of Eq. (2.2). Let us remark that, as far as we know, the observation of multicritical conformal Yukawa models at finite X_f and in continuous fractal dimensions $2 < d < 3$ is a novel result.

Concerning the finite-X_f results, they indicate that in several cases the effect of multimeson exchange cannot be neglected, either quantitatively or even qualitatively. We argued that these higher Yukawa interactions are required by consistency of the truncation; otherwise the solutions of the system of differential equations defining the flow of the scalar potential $v(\phi)$ and of the Yukawa "potential" $h(\phi)$ would depend on the chosen parametrization of these functions. For instance, the same FP solutions should be reproduced using any polynomial truncation of these functions, at least within a certain domain. On these grounds we believe that general FRG studies of Yukawa models should at least consider the inclusion of these interactions, and possibly check when they can actually be neglected.

On the quantitative side, in Sec. V we explicitly numerically constructed these global FP solutions for $d = 3$ and several values of X_f. These results include the Gross–Neveu universality class for $X_f \geq 2$ and the superconformal $\mathcal{N} = 1$ Wess–Zumino model for $X_f = 1$. At $X_f = 1$ we also numerically computed the critical exponent ν and the corresponding linear perturbation around the FP. In Sec. VI we showed how the results of the global analysis can be easily reproduced by two different kinds of high-order polynomial truncations. However, these studies were performed in the local-potential approximation, that is by neglecting the renormalization of the fields. Taking into account the anomalous dimensions (LPA′) was crucial to obtain a more accurate picture, especially for $X_f > 1$, so that in Sec. VI B we developed a LPA′ analysis, based on the same polynomial truncations which were proved to be trustworthy in the LPA studies.

This allowed us to produce estimates of the critical exponents ν, η_ϕ, and η_ψ, in $d = 3$ and various X_f and to compare them with some of the existing literature. We concentrated on the especially interesting cases of two and one massless Dirac ($X_f = 8$ and 4), of a Weyl ($X_f = 2$), and of a Majorana spinor ($X_f = 1$). They can be found in Tables X, XI, XII, and XIII. Often, there still exists some significant mismatch among the available estimates, such that more studies by all kinds of methods, including Monte Carlo simulations and higher-order ϵ or $1/N_f$ expansions, are welcome. As far as the FRG is concerned, the results seem stable for $X_f \geq 4$, while for a lower number of fermions, there is still room for debate, and probably larger truncations are needed. The supersymmetric case $X_f = 1$ is an exception also in this sense, since it enjoys a good agreement among the results produced with different methods.

Larger truncations, such as a next-to-leading order of the derivative expansion, are anyway needed for a quantitative analysis of multicritical models in $2 < d < 3$, as we argue in Appendix III in the large-X_f limit. Still within the LPA′, the next natural step is to produce global numerical studies similar to the ones presented for the LPA in Secs. IV and V. Regarding the possible applications of the present analysis to different models, one possibility is to enlarge the symmetry group from $\mathbb{Z}_2$ to $O(\mathrm{N})$. The $\mathrm{N} = 3$ three-dimensional chiral Heisenberg universality class, for instance, can be interesting for the physics of electrons in graphene [18]. With an enlarged symmetry, the effect of different representations would become a natural case study and would further widen the class of physical applications of these studies [48]. Furthermore, larger symmetry groups could lead to other interesting playgrounds for describing supersymmetric FPs within a supersymmetry-breaking FRG scheme. In particular, supersymmetric FRG studies of $O(\mathrm{N})$ models [49] provide a stimulating challenge for future generalizations of the present work. A truncation similar to the one discussed in this paper can also be used in the context of a Yukawa model interacting with gravity, along the lines of Ref. [50], to investigate first the asymptotic safety properties of the model and then to construct global flows from the UV to the IR. Some scenarios could be of particular interest for cosmology.

ACKNOWLEDGMENTS

We would like to thank Alessandro Codello, Stefan Rechenberger, Michael Scherer, and René Sondenheimer for inspiring discussions and Julia Borchardt, Tobias Hellwig, Benjamin Knorr, and Omar Zanusso for providing us some of their results, which can be found in

Sec. VI B, as well as for valuable comments. We are grateful to Holger Gies for several explanations and suggestions and for a critical reading of the manuscript. L. Z. acknowledges support by the DFG under Grant No. GRK1523/2.

APPENDIX A: REGULATORS AND THRESHOLD FUNCTIONS

We have to evaluate the rhs of Eq. (2.1), for which we need the $\Gamma_k^{(2)}$ matrix. Considering the field ψ as a column and $\bar\psi$ as a row vector, let us denote by $\Phi^{\mathrm{T}}(q)$ the row vector with components $\phi(q)$, $\psi^{\mathrm{T}}(q)$, and $\bar\psi(-q)$ and by $\Phi(p)$ the column vector given by its transposition. Then $\Gamma_k^{(2)}$ is obtained by the formula

$$\Gamma_k^{(2)} = \frac{\vec{\delta}}{\delta\Phi^{\mathrm{T}}(-p)}\Gamma_k\frac{\overleftarrow{\delta}}{\delta\Phi(q)}.$$

This inverse propagator is regularized by the addition of the regulator

$$R_k(q,p) = \delta(p-q)\begin{pmatrix} R_{\mathrm{B}}(p) & 0 \\ 0 & R_{\mathrm{F}}(p)\end{pmatrix},$$

where

$$R_{\mathrm{B}}(p) = Z_\phi p^2 r_{\mathrm{B}}(p^2),$$
$$R_{\mathrm{F}}(p) = -\begin{pmatrix} 0 & \delta^{ij}\not{p}^{\mathrm{T}} \\ \delta^{ij}\not{p} & 0\end{pmatrix} Z_\psi r_{\mathrm{F}}(p^2)$$

is a $2d_\gamma N_f \times 2d_\gamma N_f$ matrix. In principle one can have different regulators for the scalar (B) and for the spinors (F). A compact way to rewrite the flow equation is

$$\partial_t\Gamma_k = \frac{1}{2}\tilde\partial_t \mathrm{STr}\log(\Gamma_k^{(2)} + R_k),$$

where

$$\tilde\partial_t \equiv \frac{\partial_t(Z_\phi r_{\mathrm{B}})}{Z_\phi}\cdot\frac{\delta}{\delta r_{\mathrm{B}}} + \frac{\partial_t(Z_\psi r_{\mathrm{F}})}{Z_\psi}\cdot\frac{\delta}{\delta r_{\mathrm{F}}}$$

and $\cdot$ denotes multiplication as well as integration over the common argument of the shape functions of the two factors. Then the regularized kinetic (or squared kinetic) terms are given by $P_{\mathrm{B}}(x) = x(1 + r_{\mathrm{B}}(x))$ and $P_{\mathrm{F}}(x) = x(1 + r_{\mathrm{F}}(x))^2$, and the loop momentum integrals appearing on the rhs of the flow equation give rise to corresponding regulator dependent threshold functions. Introducing the abbreviation $\int_p \equiv \int \frac{d^d p}{(2\pi)^d}$, these threshold functions read

$$l_0^{(\mathrm{B/F})d}(\omega) = \frac{k^{-d}}{4v_d}\int_p \tilde\partial_t \log\left(P_{\mathrm{B/F}} + \omega k^2\right)$$
$$l_1^{(\mathrm{B/F})d}(\omega) = -\frac{k^{2-d}}{4v_d}\int_p \tilde\partial_t \frac{1}{P_{\mathrm{B/F}} + \omega k^2}$$
$$l_{n_1,n_2}^{(\mathrm{FB})d}(\omega_1,\omega_2) = -\frac{k^{2(n_1+n_2)-d}}{4v_d}\int_p \tilde\partial_t \frac{1}{(P_{\mathrm{F}} + \omega_1 k^2)^{n_1}(P_{\mathrm{B}} + \omega_2 k^2)^{n_2}}$$
$$m_2^{(\mathrm{F})d}(\omega) = -\frac{k^{6-d}}{4v_d}\int_p p^2\tilde\partial_t\left(\frac{\partial}{\partial p^2}\frac{1}{P_{\mathrm{F}} + \omega k^2}\right)^2$$
$$m_4^{(\mathrm{F})d}(\omega) = -\frac{k^{4-d}}{4v_d}\int_p p^4\tilde\partial_t\left(\frac{\partial}{\partial p^2}\frac{1 + r_{\mathrm{F}}}{P_{\mathrm{F}} + \omega k^2}\right)^2$$
$$m_4^{(\mathrm{B})d}(\omega_1) = -\frac{k^{6-d}}{4v_d}\int_p p^2\tilde\partial_t\left(\frac{\frac{\partial}{\partial p^2}P_{\mathrm{B}}}{(P_{\mathrm{B}} + \omega_1 k^2)^2}\right)^2$$
$$m_{1,2}^{(\mathrm{FB})d}(\omega_1,\omega_2) = -\frac{k^{4-d}}{4v_d}\int_p p^2\tilde\partial_t\left(\frac{1 + r_{\mathrm{F}}}{P_{\mathrm{F}} + \omega_1 k^2}\frac{\frac{\partial}{\partial p^2}P_{\mathrm{B}}}{(P_{\mathrm{B}} + \omega_2 k^2)^2}\right).$$

In this work we adopted the linear regulator $x r_{\mathrm{B}}(x) = (1-x)\theta(1-x)$, where $x = q^2/k^2$. For spinors this corresponds to a shape function r_{F} such that $x(1 + r_{\mathrm{B}}(x)) = x(1 + r_{\mathrm{F}}(x))^2$. For it the threshold functions can be computed analytically and give

$$l_0^{(\mathrm{B})d}(\omega) = \frac{2}{d}\frac{1-\frac{\eta_\phi}{d+2}}{1+\omega},$$
$$l_0^{(\mathrm{F})d}(\omega) = \frac{2}{d}\frac{1-\frac{\eta_\psi}{d+1}}{1+\omega},$$
$$l_1^{(\mathrm{B/F})d}(\omega) = -\frac{\partial}{\partial\omega} l_0^{(\mathrm{B/F})d}(\omega),$$
$$l_{n_1,n_2}^{(\mathrm{FB})d}(\omega_1,\omega_2) = \frac{2}{d}\left[n_1 \frac{1-\frac{\eta_\psi}{d+1}}{(1+\omega_1)^{1+n_1}(1+\omega_2)^{n_2}} + n_2 \frac{1-\frac{\eta_\phi}{d+2}}{(1+\omega_1)^{n_1}(1+\omega_2)^{1+n_2}}\right],$$
$$m_2^{(\mathrm{F})d}(\omega) = \frac{1}{(1+\omega)^4},$$
$$m_4^{(\mathrm{F})d}(\omega) = \frac{1}{(1+\omega)^4} + \frac{1-\eta_\psi}{(d-2)(1+\omega)^3} - \left(\frac{1-\eta_\psi}{2d-4}+\frac{1}{4}\right)\frac{1}{(1+\omega)^2},$$
$$m_4^{(\mathrm{B})d}(\omega_1) = \frac{1}{(1+\omega_1)^4},$$
$$m_{1,2}^{(\mathrm{FB})d}(\omega_1,\omega_2) = \frac{1-\frac{\eta_\phi}{d+1}}{(1+\omega_1)(1+\omega_2)^2}.$$

APPENDIX B: PROPERTIES OF THE LARGE-X_f SOLUTIONS

In both versions of the LPA, with or without $\eta_\phi = 0$, and also in the LPA′, Eq. (3.8) enables us to write the potentials in the form

$$h(\phi) = c_h \phi^n,$$
$$v(\phi) = c_v \phi^{dn} - \frac{4v_d}{d^2}\,{}_2F_1\left(1,-\frac{d}{2};1-\frac{d}{2};-c_h^2\phi^{2n}\right). \quad \text{(B1)}$$

The behavior of v for $\phi \to \pm\infty$ is

$$v_{\text{asympt}}(\phi) \simeq \left(\mathrm{sgn}(\phi)^{dn} c_v + \frac{\Gamma(-d/2)}{2^{d+1}\pi^{d/2}}|c_h|^d\right)|\phi|^{dn}, \quad \text{(B2)}$$

and, since we are assuming $2 < d < 4$, the gamma function in front of $|c_h|^d$ is positive. If $c_v \neq 0$, the scalar potential can be real only if $(-1)^{dn}$ has a real branch, that is if

$$d = \frac{m}{nj}, \qquad j \in \{1,3,5,\ldots\}, \qquad m \in \mathbb{N}, \qquad 2nj < m < 4nj. \quad \text{(B3)}$$

Its stability further requires

$$|c_h|^d \geq \frac{2^{d+1}\pi^{d/2}}{\Gamma(-d/2)} \max\{-c_v, (-1)^{1+dn}c_v\} = c_{h,\text{crit}}^d, \quad \text{(B4)}$$

and for special values of c_v and c_h, namely when $|c_h| = |c_{h,\text{crit}}|$, it can become asymptotically flat (possibly only on one side) instead of growing like ϕ^{dn}.

To understand the physical properties of the large-X_f FPs, we need to consider the RG flow in the vicinity of the corresponding critical points. In particular we consider the linearization of the flow, by looking at small fluctuations of the potentials $v = v + \delta v$, $h = h + \delta h$ and for eigenvalue solutions

$$\dot{\delta v} = -\theta\delta v, \qquad \dot{\delta h} = -\theta\delta h.$$

These equations at large X_f are extremely simple, and for the linearized regulator, they read

$$-\theta\delta v = -d\delta v + \frac{1}{n}\phi\delta v' + \frac{\delta\eta_\phi}{2}\phi v' + \frac{4v_d}{d}\frac{2h\delta h}{(1+h^2)^2} \quad \text{(B5)}$$

$$-\theta\delta h = -\delta h + \frac{1}{n}\phi\delta h' + \frac{\delta\eta_\phi}{2}\phi h'. \quad \text{(B6)}$$

In this Appendix we want to sketch a study of the properties of these FPs as well as of the linearized flow around them. We believe it can be instructive to consider separately the results obtained with or without the inclusion of the flow equation for η_ϕ. This will make evident that larger truncations, out of the reach of the present work, are necessary to get a complete picture of the large-X_f multicritical Yukawa theories.

1. LPA

If we set by hand $\eta_\phi = 0$, regardless of c_v or c_h, Eq. (3.8) leaves a discrete set of dimensions as the only possibility, the ones in Eq. (3.11). As a consequence $dn = 2(n+1)$,

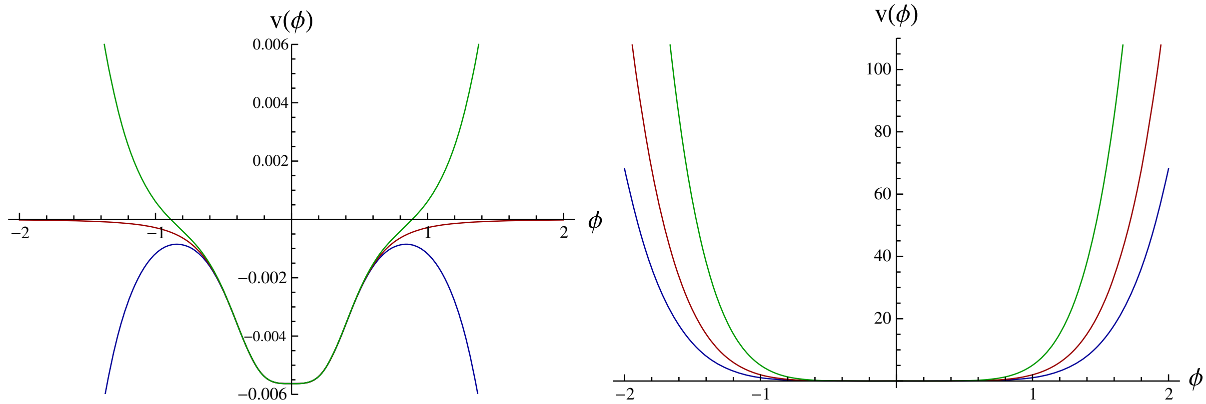

FIG. 14 (color online). The $d=3$, $n=2$, FP scalar potential at nonvanishing c_v. Left panel: $c_v=-1$ and $c_h \in \{c_{h,\mathrm{crit}}+10^{-3}, c_{h,\mathrm{crit}}, c_{h,\mathrm{crit}}-10^{-3}\}$, from bounded (green) to unbounded (blue). Right panel: $c_v=1$ and $c_h \in \{c_{h,\mathrm{crit}}+2, c_{h,\mathrm{crit}}, c_{h,\mathrm{crit}}-2\}$, from steeper (green) to broader (blue).

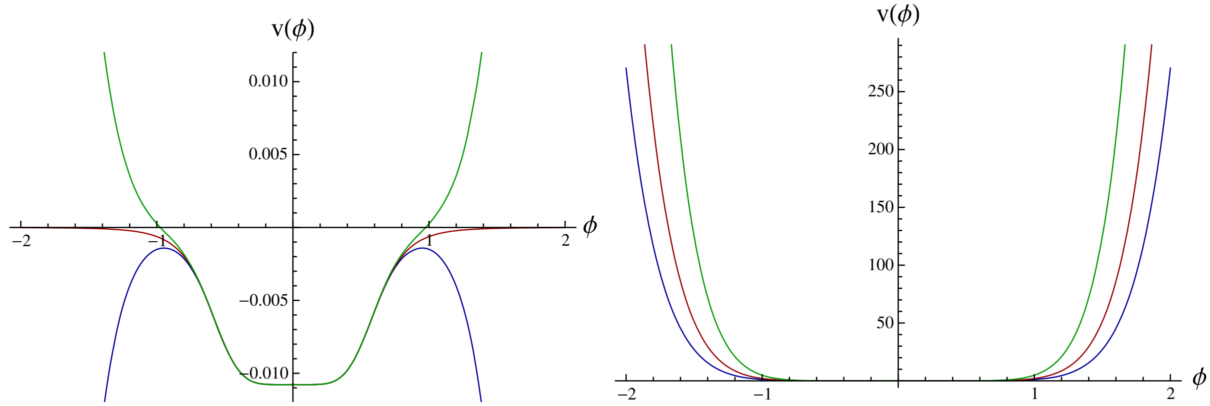

FIG. 15 (color online). The $d=8/3$, $n=3$, FP scalar potential at nonvanishing c_v. Left panel: $c_v=-1$ and $c_h \in \{c_{h,\mathrm{crit}}+10^{-3}, c_{h,\mathrm{crit}}, c_{h,\mathrm{crit}}-10^{-3}\}$, from bounded (green) to unbounded (blue). Right panel: $c_v=1$ and $c_h \in \{c_{h,\mathrm{crit}}+2, c_{h,\mathrm{crit}}, c_{h,\mathrm{crit}}-2\}$, from steeper (green) to broader (blue).

and the scalar potential is real, and even also in case $c_v \neq 0$. The stability properties, depending on c_h and c_v according to Eq. (B4), are illustrated in the plots of Figs. 14 and 15. The special case $c_v=0$ is shown in Fig. 16.

Let us now turn to the linear perturbations of these FPs. By definition in the LPA one neglects a possible change of the anomalous dimension. Thus, setting $\delta\eta_\phi=0$, the solution for the perturbations reads

$$\begin{aligned}\delta h(\phi) &= \delta c_h \phi^N\\ \delta v(\phi) &= \delta c_v \phi^{(d-1)n+N} - \frac{4v_d}{d} c_h \delta c_h \phi^{n+N}\left[\frac{1}{1+c_h^2\phi^{2n}} - \frac{d}{d-2}\,{}_2F_1\left(1, 1-\frac{d}{2}; 2-\frac{d}{2}; -c_h^2\phi^{2n}\right)\right].\end{aligned} \tag{B7}$$

Here we restricted our analysis to the perturbations with $\delta c_h \neq 0$ and required their smoothness by setting $(1-\theta)n = N \in \mathbb{N}$. For the special case $\delta c_h = 0$, the solution is simply $\delta v(\phi) = \delta c_v \phi^M$ with critical exponent $\theta_M = d - M/n$ and will not be discussed any further. Notice that these eigenfunctions are independent of c_v, which is due to the suppression of scalar loops in the large-X_f limit. They are regular at the origin, since the leading behavior is

$$\delta v(\phi) \underset{\phi\to 0}{\sim} \frac{8v_d}{d(d-2)} c_h \delta c_h \phi^{n+N}. \tag{B8}$$

Recall that the FP potential had, as leading small field dependence, ϕ^{2n}; as a consequence, the relevant

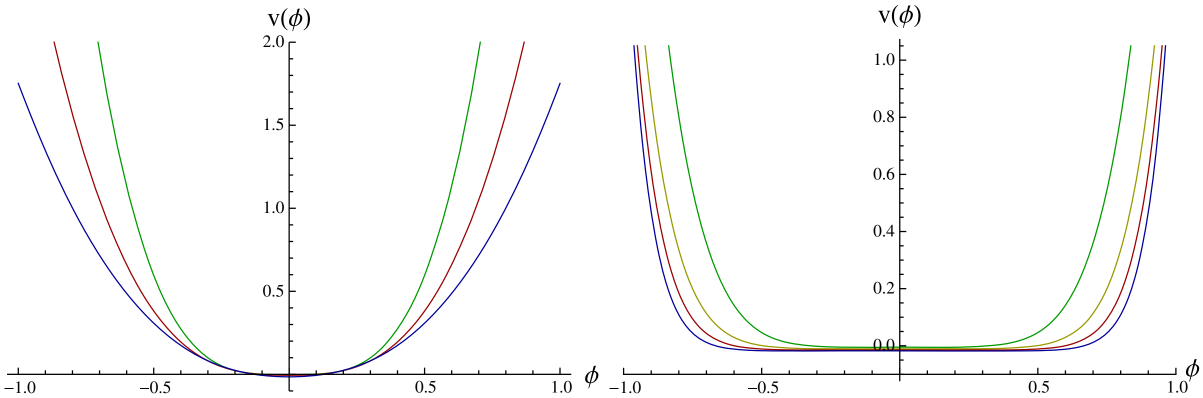

FIG. 16 (color online). The even FP scalar potentials for $c_v = 0$. For illustration the value of c_h has been chosen according to Eq. (B12), even if this is mandatory only for $n = 1$ in the LPA′. Left panel: $n = 1$ and $d \in \{3.5, 3, 2.5\}$, from steeper (green) to broader (blue). Right panel: $n \in \{2, 3, 4, 5\}$, in the corresponding dimension $d = 2 + 2/n$, from steeper (green) to broader (blue).

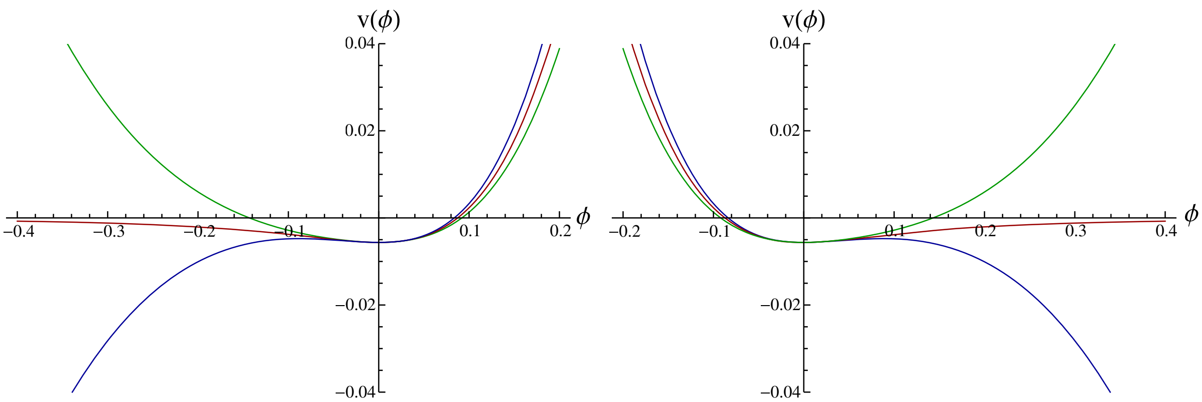

FIG. 17 (color online). The $d = 3$ and $n = 1$ FP scalar potential at nonvanishing c_v. Left panel: $c_v \in \{c_{v,\mathrm{crit}} - 1, c_{v,\mathrm{crit}}, c_{v,\mathrm{crit}} + 1\}$, from bounded (green) to unbounded (blue). Right panel: $c_v \in \{-c_{v,\mathrm{crit}} - 1, -c_{v,\mathrm{crit}}, -c_{v,\mathrm{crit}} + 1\}$, from unbounded (blue) to bounded (green). Notice that the value of the potential at the origin is arbitrary, while its behavior for large fields is not.

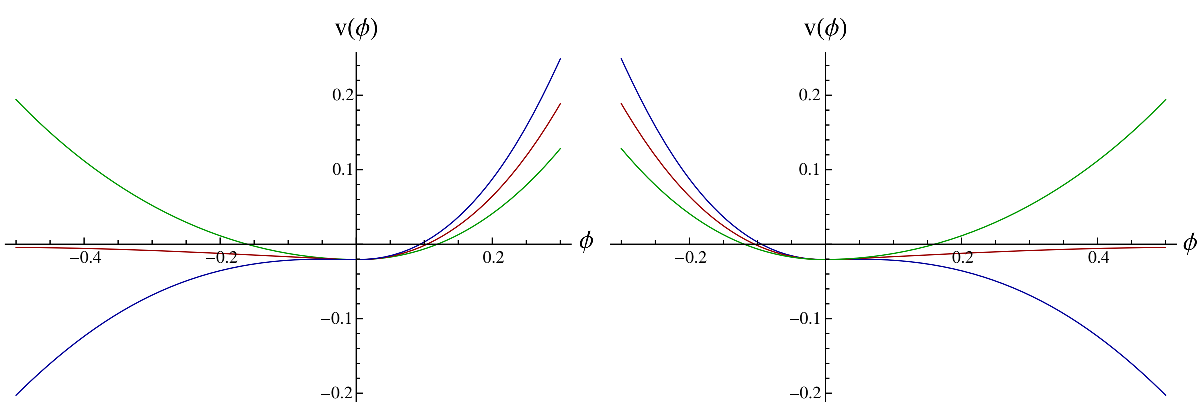

FIG. 18 (color online). The $d = 7/3$ and $n = 1$ FP scalar potential at nonvanishing c_v. Left panel: $c_v \in \{c_{v,\mathrm{crit}} - 1, c_{v,\mathrm{crit}}, c_{v,\mathrm{crit}} + 1\}$, from bounded (green) to unbounded (blue). Right panel: $c_v \in \{-c_{v,\mathrm{crit}} - 1, -c_{v,\mathrm{crit}}, -c_{v,\mathrm{crit}} + 1\}$, from bounded (green) to unbounded (blue).

perturbations with $N < n$ change the behavior of the potential at the origin, the marginal ones only change the coefficient in front of ϕ^{2n}, and the irrelevant ones leave the leading term unaltered. For a large value of the field,

$$\delta v(\phi) \underset{\phi\to\infty}{\sim} \left(\delta c_v + \mathrm{sgn}(\phi)^{dn} \frac{d\Gamma(-d/2)}{2^{d+1}\pi^{d/2}} |c_h|^{d-2} c_h \delta c_h\right) \times \phi^{dn+N-n}, \tag{B9}$$

while the FP potential behaves like $|\phi|^{dn}$ at infinity. As a consequence, the irrelevant perturbations with $N > n$ completely change the asymptotic behavior of the potential for large fields, the marginal ones with $N = n$ only change the coefficient in front of the leading power, and the relevant ones only change the subleading terms. Clearly this is not the case for those potentials, with special values of c_v, that are asymptotically flat.

Let us now discuss the symmetry properties of the perturbations. Trivially, the symmetry of Yukawa potential under $\mathbb{Z}_2$ is preserved or violated depending on n and N. We now want to understand what this entails for the scalar potential. Recall that in the LPA $dn = 2(n+1)$, and the FP v is always even. Then the fluctuations behave as ϕ^{n+N+2}, and whenever $N+n$ is odd, the $\mathbb{Z}_2$ symmetry of both h and v at the FP is spoiled by the perturbations. Among these symmetry breaking perturbations, the irrelevant ones, with $N > n$, give rise to unstable potentials. Notice that the relevant perturbations, even if spoiling symmetry, do not directly cause instabilities (though they might induce them indirectly, i.e. beyond linearization). The possibility to have stable theories with no definite $\mathbb{Z}_2$ symmetry emanating from symmetric FPs in the UV or IR is in any case a question that requires a global study of the RG flow, and it is beyond the scope of this work.

2. LPA′

So far we have not used the flow equation for η_ϕ. To do so, we first have to analyze the possible presence of a nontrivial minimum for v. The general expectation is that, since only fermion loops survive in the leading order of the $1/X_f$ expansion, the potential is always in the symmetric regime. This is suggested by the expansion of the potential around the origin, based on Eq. (3.7). We assume that this is always the case for the time being, as it is indeed for every specific example we have considered. Under this assumption, we need to take the $\phi \to 0$ limit of the equation for η_ϕ, which is proportional to $h'(\phi)^2$, i.e. to $\phi^{2(n-1)}$. Therefore, only for $n = 1$ can such a limit be nonvanishing. This shows how LPA′ is an improvement of LPA only for the $n = 1$ critical theory. For the remaining values of n, one finds again $\eta_\phi = 0$, which artificially forces the dimension d to its critical value. We expect this condition to be lifted by more general truncations, and a nontrivial η_ϕ should emerge for any n.

Let us then discuss the change brought by LPA′ in the description of the large-X_f $n = 1$ FP. As argued in Sec. III, the nontrivial η_ϕ allows for the existence of the non Gaussian FP in any $d < 4$, as long as

$$\eta_\phi = 4 - d, \qquad n = 1. \tag{B10}$$

Actually this is the case only for the $\mathbb{Z}_2$ symmetric solution with $c_v = 0$. As soon as $c_v \neq 0$ the reality of the potential requires

$$d = \frac{m}{j}, \qquad j \in \{1, 3, 5, \ldots\}, \qquad m \in \mathbb{N}, \qquad 2j < m < 4j. \tag{B11}$$

Regardless of c_v, by using Eq. (B10), the flow equation for Z_ϕ can be solved for c_h as a function of d, giving [16]

$$c_h^2 = \frac{d(4-d)(d-2)}{v_d(6d-8)}. \tag{B12}$$

Then, the stability condition Eq. (B4) for the nonvanishing c_v FPs is best phrased as a bound on c_v,

$$c_v \geq -c_{v,\mathrm{crit}}, \qquad c_{v,\mathrm{crit}} = \frac{\Gamma(-d/2)}{2^{d+1}\pi^{d/2}} \left[\frac{d(4-d)(d-2)}{v_d(6d-8)}\right]^{d/2}, \tag{B13}$$

and additionally, only for odd m, $c_v \leq c_{v,\mathrm{crit}}$. This is illustrated in Figs. 17 and 18. The scalar FP potential with $c_v \neq 0$ is an even function if and only if m is even.

Let us then turn to perturbations and allow for a nontrivial $\delta\eta_\phi$. We postpone for a while the task of solving the linearized equation for η_ϕ, which provides us the first correction $\delta\eta_\phi$ to the anomalous dimension, as a function of the FP h and δh. This is because such an equation involves the variation $\delta\phi_0$ in the location of the minimum of the potential, which in turn can be computed from the variation of the potential by the formula

$$\delta\phi_0 = -\frac{\delta v'(0)}{v''(0)}, \tag{B14}$$

where we stuck to our assumption that the minimum of the FP potential is always trivial. As a consequence we first solve for δv and δh as parametric functions of $\delta\eta_\phi$ and then plug Eq. (B14) into the linearized equation for η_ϕ, to compute the actual $\delta\eta_\phi$. Solving for δh is again trivial, and it immediately allows us to extract the eigenvalues of the linearized flow. When $\theta \neq 0$ the solution for δh is

$$\delta h(\phi) = \delta c_h \phi^N - \frac{\delta\eta_\phi}{2}\frac{n^2}{n-N} c_h \phi^n, \qquad N \in \mathbb{N}, \qquad N \neq n, \tag{B15}$$

where again we focused on $\delta c_h \neq 0$ and set $N = (1-\theta)n \in \mathbb{N}$. For $\theta = 0$ instead

$$\delta h(\phi) = \delta c_h \phi^n - \frac{\delta\eta_\phi}{2} n^2 c_h \phi^n \log(\phi). \tag{B16}$$

Notice that the second term in the last equation is simply the first order in the expansion of $c_h \phi^{2/(d-2+\eta_\phi)}$, which is the exactly marginal h, around the nth FP. As a consequence, the apparent instability that can come from the second term in Eq. (B16) is actually a fake of linearization, as long as $\delta\eta_\phi > -2/n$. On the other hand, a logarithmic singularity at the origin appears even beyond linearization, and we believe this to be a pathology produced by the leading order in $1/X_f$. The solution to this pathology will come soon, in the form of the constraint $\delta\eta_\phi = 0$ for these perturbations.

The equation for δv is much more involved in the LPA′ than in the LPA, since it now depends on the FP potential. Yet its solutions for generic $\delta\eta_\phi$ can be easily given analytically. It is not necessary to show them here. It suffices to report that quite in general they have the property $\delta v'(0) = 0$, as it could be expected by the argument that fermion loops are generally associated with scalar potentials with a trivial minimum.[4] As a consequence the scalar potential stays in the symmetric regime. Notice that this does not entail that the $\delta v(\phi)$ is also in the symmetric regime.

With this piece of information, one can work out the linearized $\delta\eta_\phi$, by varying the rhs of the flow equation for Z_ϕ with respect to h and v (the fluctuations of which still depend parametrically on $\delta\eta_\phi$ itself) and η_ϕ, while keeping ϕ_0 fixed, and then taking $\phi_0 \to 0$. The latter limit makes the rhs vanish unless $n = 1$, in which case it reaches a d-dependent constant times $c_h^2 \delta\eta_\phi$.[5] Hence, for general n and N, we find $\delta\eta_\phi = 0$, which boils the analysis of the linearized perturbations down to the one sketched in the last section within the LPA.

3. $d = 4$

The expression in Eq. (B1) cannot be used in $d = 4$ nor in $d = 2$, since the hypergeometric function in v has simple poles at these values. The $d \to 2$ case is out of the reach of the present paper. In the $d \to 4$ limit, instead, the canonical dimensional terms survive also in the LPA, and by integrating the large-X_f system of flow equations, one can find the FP solutions

$$\begin{aligned} h(\phi) &= c_h \phi^n, \\ v(\phi) &= c_v \phi^{4n} + \frac{1}{64\pi^2}\left(c_h^2 \phi^{2n} - c_h^4 \phi^{4n} \log(c_h^2 + \phi^{-2n})\right), \end{aligned} \tag{B17}$$

where we already demanded the Yukawa potential to be smooth, according to Eq. (3.8). The crucial fact is again that the minimum of v is always trivial. This allow us to take the $\phi_0 \to 0$ limit of the equation for η_ϕ. For $n = 1$ this leaves us with the equation $c_h^2 = \eta_\phi = 0$, thus boiling every feature of the critical theory down to the classical counting. For $n \geq 2$ we find the constraint $\eta_\phi = 0$, which is inconsistent with Eq. (3.8) and therefore eliminates these solutions.

[4]For $\delta c_h \neq 0$ only the $n = 1$, $N = 0$ case gives rise to a nonvanishing $\delta v'(0)$. For $\delta c_h = 0$ only the $M = 1$ case does. In what follows we discard these cases.

[5]Such a constant is actually infinite for the marginal perturbation, the rhs inheriting a logarithmic singularity at the origin from δh. Yet the simple way to cure this pathology and get a self-consistent answer is to set $\delta\eta_\phi = 0$.

[1] D. J. Gross and A. Neveu, Phys. Rev. D **10**, 3235 (1974).
[2] B. Rosenstein, B. J. Warr, and S. H. Park, Phys. Rev. D **39**, 3088 (1989); A. Kovner, B. Rosenstein, and G. Gat, Helv. Phys. Acta **65**, 411 (1992).
[3] B. Rosenstein, H. L. Yu, and A. Kovner, Phys. Lett. B **314**, 381 (1993).
[4] J. Zinn-Justin, Nucl. Phys. **B367**, 105 (1991); *Phase Transitions and Renormalization Group* (Oxford University Press, Oxford, 2007), p. 452.
[5] J. A. Gracey, Nucl. Phys. **B341**, 401 (1990); **B367**, 657 (1991); C. Luperini and P. Rossi, Ann. Phys. (N.Y.) **212**, 371 (1991).
[6] A. N. Vasiliev and M. I. Vyazovsky, Teor. Mat. Fiz. **113**, 85 (1997) [Theor. Math. Phys. **113**, 1277 (1997)]; J. A. Gracey, Nucl. Phys. **B802**, 330 (2008).
[7] J. A. Gracey, Int. J. Mod. Phys. A **09**, 567 (1994).
[8] J. A. Gracey, Int. J. Mod. Phys. A **09**, 727 (1994); A. N. Vasiliev, S. E. Derkachov, N. A. Kivel, and A. S. Stepanenko, Teor. Mat. Fiz. **94**, 179 (1993) [Theor. Math. Phys. **94**, 127 (1993)].
[9] S. Hands, A. Kocic, and J. B. Kogut, Ann. Phys. (N.Y.) **224**, 29 (1993).
[10] L. Karkkainen, R. Lacaze, P. Lacock, and B. Petersson, Nucl. Phys. **B415**, 781 (1994); **438**, 650(E) (1995).

[11] E. Focht, J. Jersak, and J. Paul, Nucl. Phys. B, Proc. Suppl. **47**, 709 (1996); S. Christofi and C. Strouthos, J. High Energy Phys. 05 (2007) 088.
[12] S. Chandrasekharan and A. Li, Phys. Rev. D **88**, 021701 (2013).
[13] L. Wang, P. Corboz, and M. Troyer, New J. Phys. **16**, no. 10, 103008 (2014).
[14] L. Rosa, P. Vitale, and C. Wetterich, Phys. Rev. Lett. **86**, 958 (2001).
[15] F. Hofling, C. Nowak, and C. Wetterich, Phys. Rev. B **66**, 205111 (2002).
[16] J. Braun, H. Gies, and D. D. Scherer, Phys. Rev. D **83**, 085012 (2011); J. Phys. A **46**, 285002 (2013).
[17] H. Sonoda, Prog. Theor. Phys. **126**, 57 (2011).
[18] L. Janssen and I. F. Herbut, Phys. Rev. B **89**, 205403 (2014).
[19] J. Borchardt and B. Knorr, arXiv:1502.07511.
[20] N. Dorey and N. E. Mavromatos, Phys. Lett. B **250**, 107 (1990); I. J. R. Aitchison and N. E. Mavromatos, Phys. Rev. B **53**, 9321 (1996); N. E. Mavromatos and J. Papavassiliou, Recent Res. Dev. Phys. Chem. **5**, 369 (2004); M. Franz and Z. Tesanovic, Phys. Rev. Lett. **87**, 257003 (2001); I. F. Herbut, Phys. Rev. Lett. **88**, 047006 (2002); Phys. Rev. B **66**, 094504 (2002); Phys. Rev. Lett. **94**, 237001 (2005).
[21] G. W. Semenoff, Phys. Rev. Lett. **53**, 2449 (1984); I. F. Herbut, Phys. Rev. Lett. **97**, 146401 (2006); I. F. Herbut, V. Juricic, and B. Roy, Phys. Rev. B **79**, 085116 (2009); V. P. Gusynin, S. G. Sharapov, and J. P. Carbotte, Int. J. Mod. Phys. B **21**, 4611 (2007); S. Hands and C. Strouthos, Phys. Rev. B **78**, 165423 (2008); J. E. Drut and T. A. Lahde, Phys. Rev. Lett. **102**, 026802 (2009); Y. Araki and T. Hatsuda, Phys. Rev. B **82**, 121403 (2010).
[22] E. V. Gorbar, V. P. Gusynin, and V. A. Miransky, Phys. Rev. D **64**, 105028 (2001); E. V. Gorbar, V. P. Gusynin, V. A. Miransky, and I. A. Shovkovy, Phys. Rev. B **66**, 045108 (2002); H. Leal and D. V. Khveshchenko, Nucl. Phys. **B687**, 323 (2004).
[23] H. Gies and L. Janssen, Phys. Rev. D **82**, 085018 (2010); L. Janssen and H. Gies, Phys. Rev. D **86**, 105007 (2012).
[24] T. Grover, D. N. Sheng, and A. Vishwanath, Science **344**, 280 (2014).
[25] L. Balents, M. P. A. Fisher, and C. Nayak, Int. J. Mod. Phys. B **12**, 1033 (1998); S. S. Lee, Phys. Rev. B **76**, 075103 (2007).
[26] Y. Nambu and G. Jona-Lasinio, Phys. Rev. **122**, 345 (1961); J. B. Kogut, M. A. Stephanov, and C. G. Strouthos, Phys. Rev. D **58**, 096001 (1998); S. Chandrasekharan, J. Cox, K. Holland, and U. J. Wiese, Nucl. Phys. **B576**, 481 (2000); S. Hands, B. Lucini, and S. Morrison, Phys. Rev. D **65**, 036004 (2002).
[27] D. U. Jungnickel and C. Wetterich, Phys. Rev. D **53**, 5142 (1996).
[28] H. Gies and M. M. Scherer, Eur. Phys. J. C **66**, 387 (2010).
[29] H. Gies, S. Rechenberger, and M. M. Scherer, Eur. Phys. J. C **66**, 403 (2010); H. Gies, L. Janssen, S. Rechenberger, and M. M. Scherer, Phys. Rev. D **81**, 025009 (2010); H. Gies, S. Rechenberger, M. M. Scherer, and L. Zambelli, Eur. Phys. J. C **73**, 2652 (2013).
[30] Y. Nambu, *Warsaw Symposium on Elementary Particle Physics: New Theories in Physics, Kazimierz, Poland, 1988*, edited by Z. Ajduk, S. Pokorski, and A. Trautman (World Scientific, Singapore, 1988), p. 1; V. A. Miransky, M. Tanabashi, and K. Yamawaki, Phys. Lett. B **221**, 177 (1989); Mod. Phys. Lett. A **04**, 1043 (1989); H. Gies, J. Jaeckel, and C. Wetterich, Phys. Rev. D **69**, 105008 (2004).
[31] O. Zanusso, L. Zambelli, G. P. Vacca, and R. Percacci, Phys. Lett. B **689**, 90 (2010); G. P. Vacca and O. Zanusso, Phys. Rev. Lett. **105**, 231601 (2010).
[32] J. M. Pawlowski and F. Rennecke, Phys. Rev. D **90**, 076002 (2014); J. Braun, L. Fister, J. M. Pawlowski, and F. Rennecke, arXiv:1412.1045.
[33] C. Wetterich, Phys. Lett. B **301**, 90 (1993); T. R. Morris, Int. J. Mod. Phys. A **09**, 2411 (1994).
[34] K. Aoki, Int. J. Mod. Phys. B **14**, 1249 (2000); J. Braun, J. Phys. G **39**, 033001 (2012); J. Berges, N. Tetradis, and C. Wetterich, Phys. Rep. **363**, 223 (2002); B. Delamotte, Lect. Notes Phys. **852**, 49 (2012); P. Kopietz, L. Bartosch, and F. Schutz, Lect. Notes Phys. **798**, 1 (2010); T. R. Morris, Prog. Theor. Phys. Suppl. **131**, 395 (1998); O. J. Rosten, Phys. Rep. **511**, 177 (2012).
[35] D. F. Litim, Phys. Rev. D **64**, 105007 (2001); Phys. Lett. B **486**, 92 (2000); Nucl. Phys. **B631**, 128 (2002); J. High Energy Phys. 11 (2001) 059.
[36] G. Felder, Commun. Math. Phys. **111**, 101 (1987).
[37] A. Codello, J. Phys. A **45**, 465006 (2012); A. Codello and G. D'Odorico, Phys. Rev. Lett. **110**, 141601 (2013); A. Codello, N. Defenu, and G. D'Odorico, Phys. Rev. D **91**, 105003 (2015).
[38] A. Hasenfratz and P. Hasenfratz, Nucl. Phys. **B270**, 687 (1986); Helv. Phys. Acta **59**, 833 (1986).
[39] T. R. Morris, Phys. Lett. B **334**, 355 (1994).
[40] T. R. Morris, Phys. Lett. B **345**, 139 (1995).
[41] T. R. Morris, Phys. Lett. B **329**, 241 (1994); T. R. Morris and M. D. Turner, Nucl. Phys. **B509**, 637 (1998).
[42] F. Synatschke, J. Braun, and A. Wipf, Phys. Rev. D **81**, 125001 (2010).
[43] M. Heilmann, T. Hellwig, B. Knorr, M. Ansorg, and A. Wipf, J. High Energy Phys. 02 (2015) 109.
[44] T. Hellwig, A. Wipf, and O. Zanusso (unpublished).
[45] H. Gies, F. Synatschke, and A. Wipf, Phys. Rev. D **80**, 101701 (2009).
[46] D. Bashkirov, arXiv:1310.8255.
[47] O. Aharony, A. Hanany, K. A. Intriligator, N. Seiberg, and M. J. Strassler, Nucl. Phys. **B499**, 67 (1997).
[48] D. Mesterhazy, J. Berges, and L. von Smekal, Phys. Rev. B **86**, 245431 (2012).
[49] M. Heilmann, D. F. Litim, F. Synatschke-Czerwonka, and A. Wipf, Phys. Rev. D **86**, 105006 (2012); D. F. Litim, M. C. Mastaler, F. Synatschke-Czerwonka, and A. Wipf, Phys. Rev. D **84**, 125009 (2011).
[50] R. Percacci and G. P. Vacca, Eur. Phys. J. C **75**, 188 (2015).